

See discussions, stats, and author profiles for this publication at: <https://www.researchgate.net/publication/316260197>

The effect of surface roughness and viscoelasticity on rubber adhesion

Article in *Soft Matter* · April 2017

DOI: 10.1039/C7SM00177K

CITATIONS

63

READS

1,895

8 authors, including:



Avinash Tiwari

Forschungszentrum Jülich

42 PUBLICATIONS 388 CITATIONS

[SEE PROFILE](#)



Leonid Dorogin

ITMO University

63 PUBLICATIONS 667 CITATIONS

[SEE PROFILE](#)



Kyle Schulze

Auburn University

28 PUBLICATIONS 791 CITATIONS

[SEE PROFILE](#)

Some of the authors of this publication are also working on these related projects:



Understanding the Friction and Wear Behavior of 2D Materials [View project](#)



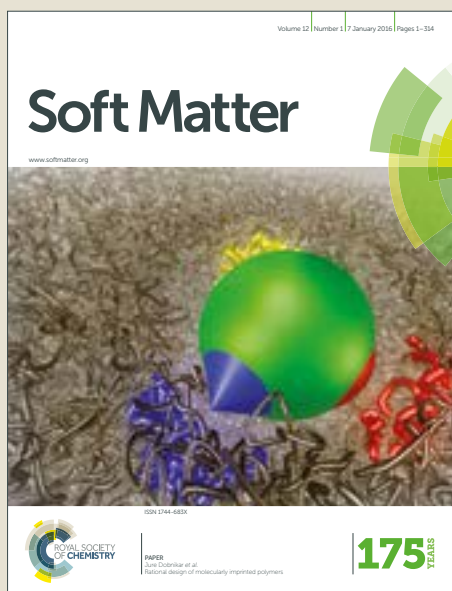
soft matter tribology [View project](#)

Soft Matter

Accepted Manuscript



This article can be cited before page numbers have been issued, to do this please use: A. Tiwari, L. Dorogin, A. I. Bennett, K. D. Schulze, W. G. Sawyer, M. Tahir, G. Heinrich and B.N.J. Persson, *Soft Matter*, 2017, DOI: 10.1039/C7SM00177K.



This is an Accepted Manuscript, which has been through the Royal Society of Chemistry peer review process and has been accepted for publication.

Accepted Manuscripts are published online shortly after acceptance, before technical editing, formatting and proof reading. Using this free service, authors can make their results available to the community, in citable form, before we publish the edited article. We will replace this Accepted Manuscript with the edited and formatted Advance Article as soon as it is available.

You can find more information about Accepted Manuscripts in the [author guidelines](#).

Please note that technical editing may introduce minor changes to the text and/or graphics, which may alter content. The journal's standard [Terms & Conditions](#) and the ethical guidelines, outlined in our [author and reviewer resource centre](#), still apply. In no event shall the Royal Society of Chemistry be held responsible for any errors or omissions in this Accepted Manuscript or any consequences arising from the use of any information it contains.

The effect of surface roughness and viscoelasticity on rubber adhesion

A. Tiwari,^{1,2} L. Dorogin,^{2,3,4} A.I. Bennett,⁵ K.D. Schulze,⁵
W.G. Sawyer,⁵ M. Tahir,³ G. Heinrich,³ and B.N.J. Persson^{*2,6}

View Article Online
DOI: 10.1039/C7SM00177K

¹*Department of Mechanical and Industrial Engineering,
Norwegian University of Science and Technology,
Richard Birkelandsvei 2B, N-7491 Trondheim, Norway*

²*PGI-1, FZ Jülich, Germany, EU*

³*Leibniz Institute for Polymer Research Dresden, P.O. Box 120 411, D-01005 Dresden, Germany*

⁴*ITMO University, Kronverskiy pr. 49, 197101, Saint Petersburg, Russia*

⁵*Department of Mechanical and Aerospace Engineering,
University of Florida, Gainesville, FL 32611, USA*

⁶*www.MultiscaleConsulting.com*

Adhesion between silica-glass or acrylic balls and silicone elastomers and various industrial rubbers is investigated. The work of adhesion during pull-off is found to strongly vary depending on the system, which we attribute to the two opposite effects: (1) viscoelastic energy dissipation close to an opening crack tip, and (2) surface roughness. Introducing surface roughness on the glass ball is found to increase the work of adhesion for soft elastomers, while for the stiffer elastomers it results in a strong reduction in the work of adhesion. For the soft silicone elastomers a strong increase in the work of adhesion with increasing pull-off velocity is observed, which may result from the non-adiabatic processes associated with molecular chain pull-out. In general, the work of adhesion is decreased after repeated contacts due to the transfer of molecules from the elastomers to the glass ball. Thus, extracting the free chains (oligomers) from the silicone elastomers is shown to make the work of adhesion independent of the number of contacts.

The viscoelastic properties (linear and nonlinear) for all of the rubber compounds were measured, and the velocity dependent crack opening propagation energy at the interface was calculated. Silicone elastomers show a good agreement between the measured work of adhesion and the predicted results, but carbon black filled hydrogenated nitrile butadiene rubber compounds reveal that strain softening at the crack tip may play an important role in determining the work of adhesion. Additionally, adhesion measurement in submerged conditions under distilled water and water+soap solutions were also performed: a strong reduction in the work of adhesion was measured for the silicone elastomers submerged in water, and a complete elimination of adhesion was found for the water+soap solution attributed to an osmotic repulsion between the negatively charged surface of the glass and the elastomer.

1 Introduction

Contact mechanics and adhesion are central topics in Tribology[1–3] with applications to tires, seals, human joints, pressure sensitive adhesives, granular matter, wiper blades and syringes, to name just a few. Contact mechanics for elastic solids with randomly rough surfaces in the absence of adhesion is now well understood[4–10]. However, with adhesion the problem becomes much more complex and is not yet fully understood[4, 11–19], in particular for real materials like rubber with viscoelastic (and non-linear) properties[20–23].

Even the weakest forces acting between the atoms in solids is strong on a macroscopic scale[24, 25]. Nevertheless, adhesion is usually not detected at the macroscopic length scale, e.g., we do not observe any adhesive forces when walking even on very smooth surfaces, unless the surfaces are contaminated with a very soft (typically viscoelastic) material like chewing gum. The reason for the negligible strength of adhesion at the macroscopic length scale is mainly due to surface roughness. Thus, surface roughness reduces the area of real contact and, more importantly, to make contact with a rough surface it is necessary to locally deform the solids at the interface; during

pull-off the stored elastic energy is given back and help to break the adhesive bonds resulting in a nearly vanishing pull-off force in most cases. In the language of the renormalization group theory, we may state that integrating out the short length-scales degrees of freedom result in the macroscopic state where adhesion usually does not manifest itself directly[26]. It is important to note, however, that even if no adhesion can be detected in a pull-off experiment, the adhesive interaction will *always* increase the area of real contact and hence will affect, e.g., sliding friction[27].

For very soft elastic solids, e.g. for soft rubber, and for very smooth surfaces, adhesion can manifest itself also at macroscopic length scales. In nature natural selection has resulted in insects, tree frogs and Gecko's having adhesive pads build in a hierarchic way from elastically stiff materials (keratin-like proteins with an elastic modulus ~ 1000 times higher than that of typical rubber materials), which are soft on all length scales, and which allow the animals to adhere even to very rough surfaces[28–30].

Adhesion is often studied using a flat cylinder punch[22, 31], but from both an experimental and theoretical point of view the simplest and most well-defined

contact mechanics problem is the contact between a ball (radius R) and a flat surface. For this problem two limiting cases can be solved exactly, namely the case of an elastically soft contact with large radius R , where the Johnson–Kendall–Roberts (JKR)[32, 33] theory is valid, and that of an elastically hard contact with small radius R , where the Derjaguin–Muller–Toporov (DMT)[34] theory is valid. The contact between elastic solids with random roughness on many length scales is a much more complex topic, involving asperities with radius of curvature extending over many decades in length scale. In this case the contact mechanics may appear DMT-like at short length scales and JKR-like at long length scales. Using the language of the renormalization group theory, as we integrate out length scales we may pass from a DMT-like picture at short length scale, where the contact mechanics depends on the detailed nature of the interaction potential between the atoms, to a JKR-like picture at longer length scale, where the detailed nature of the interaction potential is unimportant, and where just the work of adhesion (which now depends on the length scale) matters, to the macroscopic limit where perhaps the adhesion (as manifested as a pull-off force) vanishes.

In the present study we consider the adhesion between rubber materials and smooth (and rough) counter surfaces. We study the adhesion between glass and acrylic balls, and several types of rubbers. The surface energies of all the rubbers are very similar, but we find that the work of adhesion during pull-off varies over several orders of magnitude. This is remarkable because in the adiabatic (i.e., infinitesimally low pull-off velocity) limit the work of adhesion for smooth surfaces should be equal to the change in the interfacial free energy $\Delta\gamma = \gamma_1 + \gamma_2 - \gamma_{12}$ (where γ_1 , γ_2 and γ_{12} is the solid-vapor interfacial energies of solid 1 and 2, and the interfacial energy of the contact between solid 1 and 2, respectively), which is expected to change very little between the different systems[3]. We show that the strong variation in the work of adhesion is due to two competing effects: non-adiabatic effects, in particular the viscoelastic energy dissipation in the vicinity of the opening crack tip[23, 43], which tend to strongly increase the work of adhesion, and the influence of surface roughness which tends to reduce the work of adhesion[44]. For the soft silicone elastomers studied below there appear to be still another contribution to the work of adhesion, which increases strongly with the crack tip velocity. This contribution may have a similar origin as for pressure sensitive adhesives, involving, e.g., cavitation and stringing[22], but visual inspection of the contact region does not support this conclusion. We instead believe it is due to non-adiabatic processes associated with chain pull-out.

This paper is organized as follows: In Sec. 2 we present a short review of the JKR-theory which is used to analyze the experimental data. In particular we show how the (opening) crack tip velocity v_r can be determined

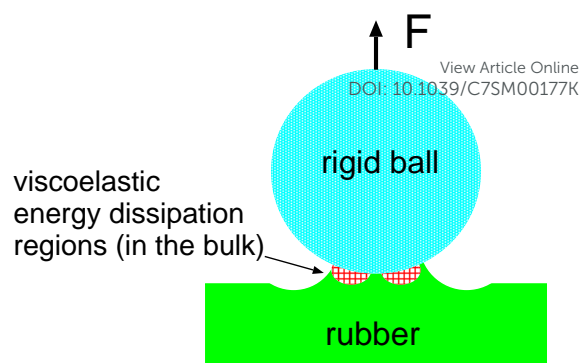


FIG. 1: A rigid ball pulled away from a viscoelastic solid. A part of the energy needed to remove the ball is derived from the viscoelastic energy dissipation inside the rubber close to the opening crack tip (red dashed region).

from the time-dependency of the interaction force $F(t)$ and pull-off displacement $\delta(t)$. The crack tip velocity is needed for the determination of the viscoelastic contribution to the crack propagation energy (or work of adhesion) (see Sec. 4.5), and also the nature of the bond-breaking in the crack tip process zone depends on this velocity. In Sec. 3 we briefly describe the two experimental set-up used for the adhesion studies. In Sec. 4.1 we study adhesion using an acrylic ball in contact with Polydimethylsiloxane (PDMS). The contact is studied using an optical microscope and the time dependency of the contact radius is measured and found to be in good agreement with the JKR prediction. This result is very important because in the second experimental set-up no direct observation of the contact was possible, but based on the success of the JKR theory for the acrylic ball we used the JKR theory to calculate v_r from the time dependency of the pull-off force. In Sec. 4.2-4.6 we present experimental results for a silica glass ball in contact with PDMS. The influence of surface roughness is studied in Sec. 4.3 using a sandblasted glass ball. The dependency of the work of adhesion on the waiting time (time of stationary contact) is shown in Sec. 4.4. The dependency of the work of adhesion on the crack tip velocity is studied in Sec. 4.5 for PDMS. In Sec. 4.6 we study the adhesion for PDMS with extracted oligomers. In Sec. 4.7 we describe adhesion between glass and PDMS in water and in water + soap. In Sec. 5 we present experimental results and theory analysis for the adhesion between the glass ball and several different types of rubber: Acrylonitrile Butadiene Rubber (NBR), Ethylene Propylene Diene (EPDM) and polyepichlorohydrin (GECO) (Sec. 5.1), and Hydrogenated Nitrile Butadiene Rubber (HNBR) with various amount of carbon black filler (Sec. 5.2). The paper is finalized with the summary and conclusions in Sec. 6.

2 Short review of the Johnson–Kendall–Roberts theory

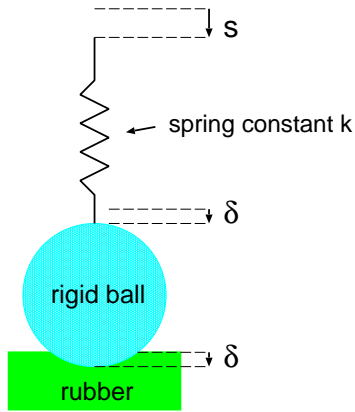


FIG. 2: If the spherical body can be treated as rigid, the penetration δ is equal to the displacement of the uppermost point of the ball towards the substrate where $\delta = 0$ corresponds to the case when the ball just touches the (undeformed) substrate in one point. Often δ is not measured directly but rather the displacement s further away and in this case some elastic element (spring constant k) relates the displacements δ and s via $k(s - \delta) = F$, where F is the force exerted by the ball on the substrate.

The analysis of the experimental data is based on the JKR theory[32]. The contact region between a spherical probe (radius R) and a flat rubber surface is circular with the radius r . The interaction between the solids is described by the work of adhesion w , which is the energy per unit surface area necessary to separate two flat surfaces from their equilibrium contact position to infinite separation. According to the JKR theory the relation between the force F and the radius r on the stable branch of the interaction curve is

$$r^3 = \frac{3RF_c}{4E^*} \left[\frac{F}{F_c} + 2 + 2 \left(\frac{F}{F_c} + 1 \right)^{1/2} \right], \quad (1)$$

where $E^* = E/(1 - \nu^2)$, and E and ν are the rubber's Young's modulus and Poisson ratio, respectively, and

$$F_c = \frac{3\pi}{2} wR \quad (2),$$

is the maximum pull-off force. Thus for an elastic solid, if the ball is pulled by a soft spring (and neglecting inertia effects), at $F = -F_c$ the pull-off force abruptly drops to zero.

It is well known that the the separation line $r = r(t)$ can be considered as a crack tip. The work of adhesion w in general depends on the velocity $v_r = \dot{r}$ of the opening (during pull-off) or closing (during contact formation) crack. At finite crack velocity, for an opening crack w can be strongly enhanced, and for a closing crack strongly reduced, compared to the adiabatic (infinitely low crack tip velocity) value w_0 . One contribution to the work of adhesion is derived from the viscoelastic energy dissipation in the vicinity of the crack tip (see Fig. 1). For an opening

crack this will enhance w with a factor $1 + f(v_r, T)$, which depend on the crack tip velocity v_r and the temperature T . For a closing crack the corresponding reduction factor is approximately $\approx 1/(1 + f(v_r, T))$ as described in [45].

The JKR theory assumes elastic solids, and it is not clear a priori if it can be applied to viscoelastic solids like rubber. However, if the elastic deformation field far away from the crack can be treated as elastic, and if the pull-off velocity is not too high, one expects the JKR theory to hold also for viscoelastic solids.

We have performed two sets of experiments using two different set-ups. At the University of Florida (UF) the probe ball is an acrylic ball with diameter 0.635 cm which is brought into contact with the substrate using an approximately rigid drive. In this set-up we could study the contact region optically and determine the radius of contact $r(t)$ directly. In the Jülich set-up the probe ball is a soda-lime silica glass ball with diameter 4 cm (dry surfaces) or 2.5 cm (in fluids). In this case the drive can be represented by a relatively soft spring (see Fig. 2), and the contact region is not observed directly but only the time dependency of the interaction force $F(t)$, and the displacement $s(t)$ of the upper part of the driving spring, are measured.

Since the work of adhesion depends on the crack tip velocity $v_r = \dot{r}(t)$ we need to determine this quantity. In the UF experiments it can be obtained directly since the time-dependency of the radius $r(t)$ is measured optically. In the Jülich experiments we calculate v_r from the time dependency of $F(t)$ assuming that the JKR theory is valid. Thus using (1) we can obtain $r(t)$ from the measured $F(t)$. During pull-off the velocity v_r varies with time, but what is most important is the velocity at the point when the pull-off force is maximal; this is the crack velocity quoted below.

There is a second way one can derive the velocity v_r , namely from the time dependency of the vertical displacement of the drive. Thus using the JKR relation between the penetration δ and the radius r of the contact region,

$$\delta = \frac{r^2}{R} - \left(\frac{2\pi w r}{E^*} \right)^{1/2}, \quad (3)$$

one can show that at pull-off ($F = -F_c$)[20]

$$v_r = \left(\frac{9R^2 E^*}{16F_c} \right)^{1/3} \dot{\delta}. \quad (4)$$

However, this equation can be used only if the penetration $\delta(t)$ is known. If the drive is rigid (or stiff enough) $\delta(t)$ is equal (or near equal) to the drive displacement $s(t)$. This is the case in the UF set-up, but not in the Jülich set-up where an effective spring separate the drive from the glass ball (see Fig. 2). If the spring constant is denoted by k , then $k(s - \delta) = F$.

We have tested the JKR theory predictions above using the UF set-up where $r(t)$ was measured directly (see

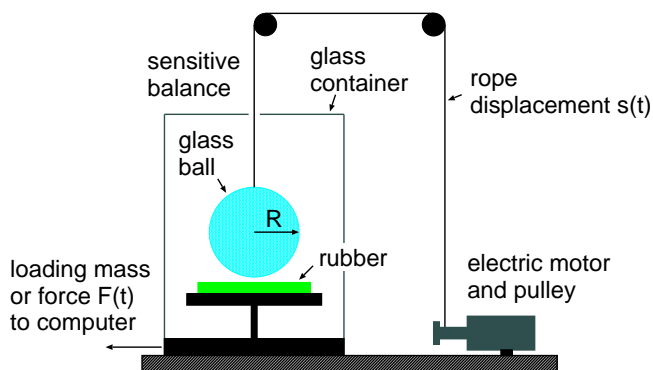


FIG. 3: The Jülich experimental set-up for measuring adhesion.

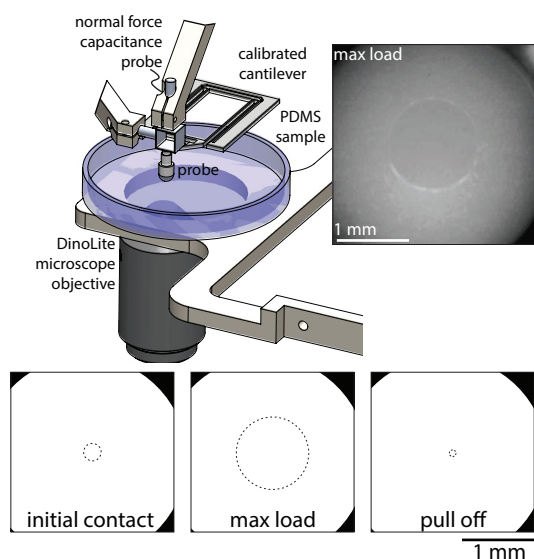


FIG. 4: The University of Florida experimental set-up for measuring adhesion, and optical images of the contact.

Sec. 4.1). We find good agreement between the experiments and the JKR theory prediction. Thus, in analyzing the experiments performed in Jülich we have obtained v_r from the time dependency of the interaction force $F(t)$ using (1).

3 Experimental

We have studied the adhesion interaction between spherical bodies (balls) and rubber. The balls are made from silica glass (Jülich lab) or acrylic polymer (UF lab). In the UF experiments the substrates were Polydimethylsiloxane (PDMS) with different crosslink density. The same substrates were used in the Jülich experiments, but here we also studied adhesion against several other types of rubber.

In the experiments performed in Jülich we brought a glass ball (with diameter $2R \approx 4$ cm) into contact with a rubber substrate as shown in Fig. 3. It is positioned on a very accurate balance (analytical balance produced by

Mettler Toledo, model MS104TS/00) which has a reproducibility of 0.1 mg (or $\approx 1 \mu\text{N}$). After zeroing the scale of the instrument we can measure the force on the substrate as a function of time which is directly transferred to a computer at a rate of 1 sample per second.

To move the glass ball up and down we have used an electric motor coiling up a nylon cord, which is attached to the glass ball. The pulling velocity as a function of time can be specified on a computer. In the experiments reported on below the glass ball is repeatedly moved up and down, for up to ~ 20 contact cycles, involving a measurement time of up to 70 hours. Fig. 7 below shows a typical force-time curve during one contact cycle.

The second experiment (at UF) involves micro adhesion experiments with in situ contact observation (see Fig. 4). An optical in situ microtribometer [21] was used for micro-scale adhesion experiments. The tribometer (see Fig. 4) was used to perform load-unload experiments between an acrylic ball (with diameter $2R \approx 0.635$ cm) and flat sheets of PDMS elastomer. The ball is fixed to the end of a cantilever force transducer with deflection monitored by capacitance probes. The probe is lowered into and raised out of contact using a piezoelectric stage. Externally applied load is measured with resolution of better than $1 \mu\text{N}$, and is linearly proportional to the displacement of the capacitance probe; ball penetration δ is monitored by subtracting the cantilever deflection from the piezoelectric stage position. Images of the contact between the acrylic ball and the PDMS elastomer, see Fig. 4, are acquired at 2 images per second and synched with force and position data. The images are processed to calculate the radius of contact $r(t)$ as a function of time t .

The equipments we used to measure the pull-off force are highly accurate, and can resolve forces of order $1 \mu\text{N}$, while the smallest pull-off force we measure is of order 1 mN, i.e., 1000 larger than the instrumental resolution. However, the balance used in the Jülich experiments gives the load (or normal force) only as 1 data point per second and in some cases, where the negative force occur over a short time period (say a few seconds), this introduce an uncertainty in the measured pull-off force, and it is the origin of the “noise” which can be observed in Fig. 17 for the highest pull-off speeds. In addition to this uncertainty, which occurred in just a few (high speed) measurements, there is an uncertainty in the results presented below due to fluctuations in the surface conditions like surface roughness and contamination. These uncertainties can only be studied by repeating the experiments several times. We did do so in some cases, see e.g. the inset in Fig. 8, where we show results when adhesion tests was performed on some PDMS compounds 2 month after performing the original measurements reported on in this figure.

In the study below we have used many types of rubber but the main focus is on PDMS elastomers which was

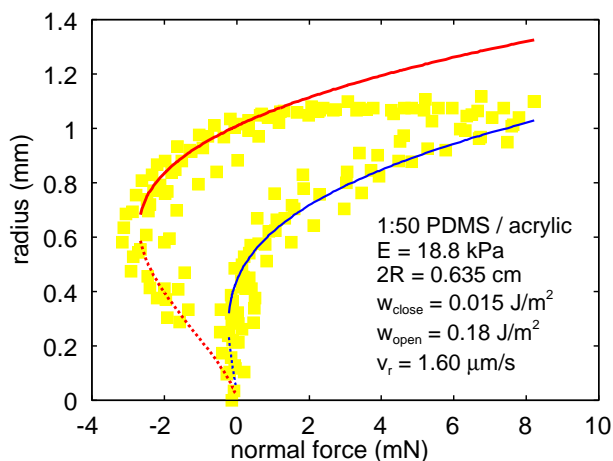


FIG. 5: The radius of the contact region as a function of normal force for an acrylic spherical probe (diameter $2R = 0.635$ cm) during approach and retraction from a 1:50 Sylgard elastomer. The yellow squares are measured data during 5 contact cycles, and the blue and red lines are the JKR fit during retraction and approach, respectively. The dotted lines are the unstable branch of the JKR adhesion curves. The fit use the Young's elastic modulus $E = 18.8$ kPa and the work of adhesion $w = 0.18$ J/m² (retraction) and $w = 0.015$ J/m² (approach). The drive velocity $v_z = \pm 0.475$ μ m/s and the crack tip velocity when the pull-off force is maximal $v_r = 1.78$ μ m/s.

produced from Sylgard 184. This is a two-component kit purchased from Dow Corning (Midland, MI) consisting of a base (vinyl-terminated polydimethylsiloxane) and a curing agent (methylhydrosiloxane-dimethylsiloxane copolymer) with a suitable catalyst. From these two components we prepared mixtures 1:10, 1:20, 1:30, 1:40 and 1:50 (cross-linker/base) in weight. The mixture was degassed to remove the trapped air induced by stirring from the mixing process and then poured into the cast. The samples were cured in an oven at 80°C for 14 h.

We note that even after curing the samples still have free polymer chains in the bulk who can move (diffuse) to the surface of the PDMS ball and hence influence the adhesion interaction. It is possible to remove a large fraction of these free chains by swelling in hexane. In our earlier study[20] we found that for the 1:10 compound the weight of the elastomer was reduced by $\approx 3.6\%$ upon extracting the free chains. For the 1:10 compound used below we found a similar mass reduction, namely $\approx 4.0\%$. The other elastomers with smaller cross-linker/base ratio will contain even more uncrosslinked polymer chains, and for the 1:50 compound we found the weight of the elastomer was reduced by $\approx 40.4\%$. In fact, the 1:50 sample broke up into small fragments during the swelling and following drying process.

4 Experimental results for Polydimethylsiloxane

4.1 Acrylic ball

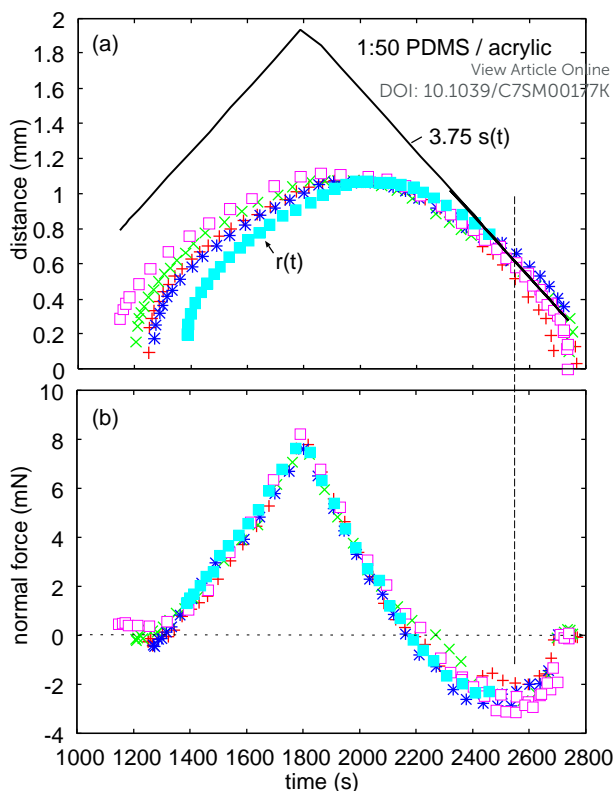


FIG. 6: (a) The radius of the contact region $r(t)$ (red, green and blue symbols) and the displacement of the drive $s(t)$ (black line) scaled by a factor of 3.7, as a function of time. The displacement of the drive $s(t)$ curve was shifted vertically so as to overlap the measured data close to pull-off. (b) The normal force $F(t)$ as a function of time. The adhesion experiment was repeated 5 times and the different symbols refer to the different measurements. For the PDMA 1:50 elastomer under the conditions given in Fig. 5.

We first consider the measured adhesion data obtained using the UF set-up. In these experiments an acrylic ball was moved in and out of contact 5 times. Before each such measurement sequence the acrylic ball was cleaned with ethanol.

The contact area was studied optically and the contact radius $r(t)$ was measured. Hence we can compare the velocity $v_r = \dot{r}(t)$ with the JKR predictions using either the measured time dependence of the force $F(t)$, from which we can calculate $r(t)$ from (1), or from the known pull-off velocity $v_z = \dot{s} \approx \dot{\delta}$ using (3). In particular we are interested in the velocity v_r when the pull-off force is maximal.

The JKR theory was developed for an elastic solid, so the most problematic case is the PDMS 1:50 as this has the strongest dissipative characteristics. In Fig. 5 we show the radius of the contact region as a function of normal force for an acrylic spherical probe (diameter $2R = 0.635$ cm) during approach and retraction from a 1:50 Sylgard elastomer. The yellow squares are the

TABLE I: The Young's modulus E , the work of adhesion during approach w_{close} and during retraction w_{open} the pull-off velocity v_z , and the opening crack tip velocity v_r at the point where the adhesion force is maximal. The latter is obtained directly from the $r(t)$ -data (method [1]) and from (4) (method [2]). The adhesion data are for an acrylic ball in contact with PDMS 1:10, 1:20, 1:30, 1:40 and 1:50 compounds.

Compound	1:10	1:20	1:30	1:40	1:50
E [MPa]	2.3	0.75	0.25	0.068	0.019
w_{close} [J/m ²]	0.012	0.012	0.012	0.013	0.015
w_{open} [J/m ²]	0.08	0.10	0.15	0.18	0.18
v_z [$\mu\text{m/s}$]	0.108	0.154	0.208	0.231	0.475
$v_r[1]$ [$\mu\text{m/s}$]	2.39	2.40	1.97	1.34	1.78
$v_r[2]$ [$\mu\text{m/s}$]	2.64	2.41	1.97	1.33	1.79

measured data, and the blue and red lines are the JKR fit curves during retraction and approach, respectively. The dotted lines are the unstable branch of the JKR adhesion curves. In the JKR fit we used the Young's elastic modulus $E = 18.8$ kPa and the work of adhesion $w = 0.18$ J/m² (retraction) and $w = 0.015$ J/m² (approach). The Young's modulus obtained from the JKR fit is in relative good agreement with the Dynamic Mechanical Analysis (DMA) study presented below (see Sec. 4.5).

In the present experiments the normal drive velocity $v_z = \pm 0.475$ $\mu\text{m/s}$ and using (from Fig. 5) $E^* = E/(1 - \nu^2) \approx 25$ kPa (where we have used that for rubber materials the Poisson ratio $\nu \approx 0.5$) and the measured pull-off force, $F_c \approx 2.7$ mN, from (4) we get $v_r = 3.75v_z \approx 1.79$ $\mu\text{m/s}$. This value is very close to the value we obtain directly from the measured $r = r(t)$. Thus in Fig. 6(a) we show the measured time dependency of contact radius $r(t)$, and of the displacement of the drive $s(t)$, scaled by a factor of 3.75. The displacement of the drive curve was shifted vertically so as to overlap the measured $r(t)$ -data close to pull-off. The adhesion experiment was repeated 5 times and the different symbols refer to the different measurements. The pull-off velocity is $v_z = \dot{s}(t) \approx 0.475$ $\mu\text{m/s}$. Note that to within the accuracy of the experiment, the relation $v_r = 3.75v_z$ is well obeyed close to the time $t = t_c$ where the pull-off force is maximal (indicated by the vertical dashed line in Fig. 6). Using $v_z = 0.475$ $\mu\text{m/s}$ we get $v_r \approx 1.78$ $\mu\text{m/s}$, which is close to the value 1.79 $\mu\text{m/s}$ obtained from (4). It is interesting to note that the opening crack velocity $v_r = \dot{r}(t)$ is close to 1.78 $\mu\text{m/s}$ also on a large part of the unstable branch of the pull-off curve (i.e., for $t > t_c$).

In Fig. 6(b) we show the normal force $F(t)$ as a function of time. It is interesting to note that while the normal force is largest at the time where the indentation is largest, the radius of the contact area is maximal about

200 s later. This is due to the viscoelastic nature of the elastomer. Thus, the JKR theory is not exact in the present context, but for our purpose the deviations between theory and experiments are unimportant.

In Table I we summarize the results obtained by analyzing the measured data for all the PDMS compound. The Young's modulus and work of adhesion was obtained by fitting the measured data to the JKR prediction as in Fig. 5. The velocity of the opening crack at the point where the adhesion force is maximal was obtained from the dependency of $r(t)$ on time (method [1]), as in Fig. 6(a) for the 1:50 compound, or from (4) (method [2]). We note that the w_{open} and w_{close} are rather uncertain, in particular for compounds 1:10 and 1:20, due to the noise in the measured data. The results in Table I will be discussed later.

4.2 Glass ball

We now present the results obtained using the experimental set-up in Jülich. Fig. 7 shows the interaction force as a function of time between an originally clean glass ball and the Sylgard PDMS elastomer with composition 1:30. In (a) we show a cycle of 5 contacts. In (b) we show a magnified view of contact 3 (dashed rectangle in (a)) and in (c) we show contact during approach (dashed rectangle in (b)). The drive velocity is $v_z = 0.87$ $\mu\text{m/s}$ and the crack tip velocity when the pull-off force is maximal $v_r = 5.1$ $\mu\text{m/s}$. Note that the pull-off force decreases with the number of contacts.

The work of adhesion (obtained from (2)) during retraction (separation) is shown in Fig. 8 as a function of the number of contacts for all the PDMS compounds. The glass ball was originally cleaned with acetone but due to surface contamination by the uncrosslinked PDMS molecules, the adhesion decreases with the number of contacts. The effect is very large for the 1:50, 1:40 and 1:30 compound but rather small for the 1:20 and 1:10 compounds. Note also that it appears that for the 1:30 compound the work of adhesion will reach its asymptotic (large contact number) value after about 20 contacts.

To test the reproducibility of the results presented above, the insert in Fig. 8 shows the work of adhesion during retraction (separation) as a function of the number of contacts for the 1:10 and 1:50 PDMS compounds. The red and blue circles are results obtained 2 month later using a new prepared PDMS sample and a new, nominally identical, glass ball. The thickness of the PDMS slab was ≈ 4 mm in the first experiment (red squares) and ≈ 8 mm in the second experiment. In addition the experiments was performed at different (unknown) humidity's and at slightly different temperatures in the range $(20 \pm 2)^\circ\text{C}$. The glass balls were cleaned with acetone before each measurement sequence. In spite of these differences in the experimental conditions the agreement between the two set of measurements is very good.

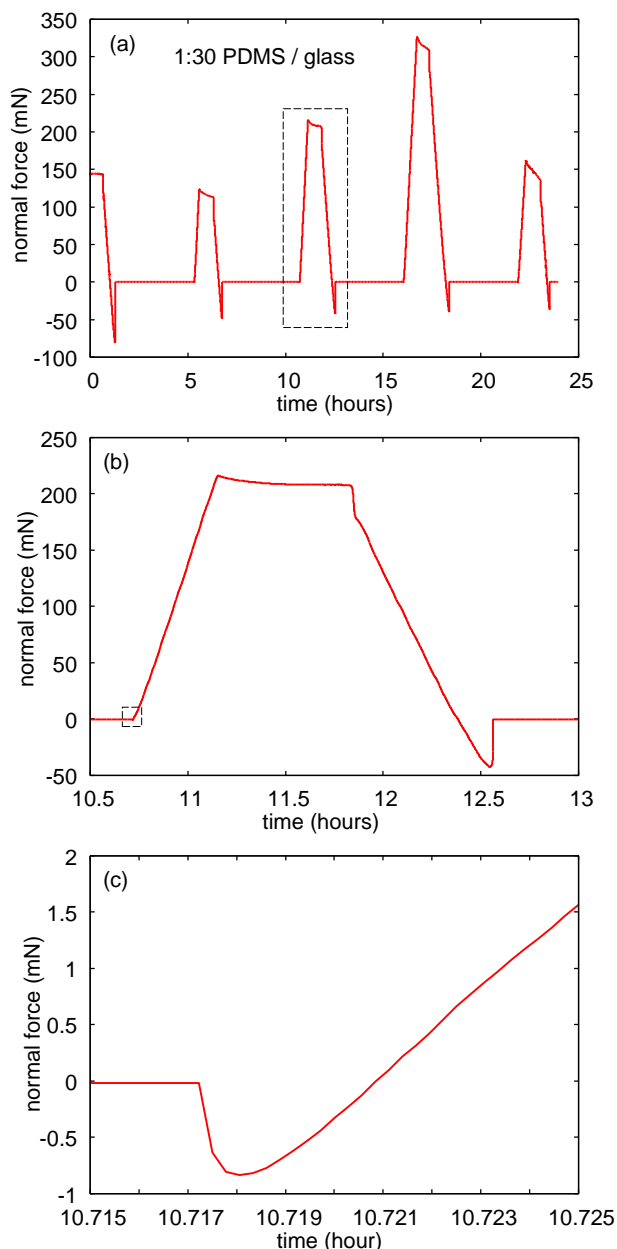


FIG. 7: The interaction force as a function of time between an originally clean glass ball and the Sylgard PDMS elastomer with composition 1:30. In (a) we show a cycle of 5 contacts. In (b) we show a magnified view of contact 3 (dashed rectangle in (a)) and in (c) we show contact during approach (dashed rectangle in (b)). The drive velocity is $v_z = 0.87 \mu\text{m/s}$ and the crack tip velocity, when the pull-off force is maximal, $v_r = 5.1 \mu\text{m/s}$.

Before each measurement sequence, where we study repeated contact between the glass ball and the PDMS surface, we clean the glass ball with acetone. For the 1:30, 1:40 and 1:50 compounds we find that the work of adhesion drops strongly with the number of contacts (see Fig. 7 and 8). We interpret this as resulting from transfer of uncrosslinked (free) PDMS molecules to the

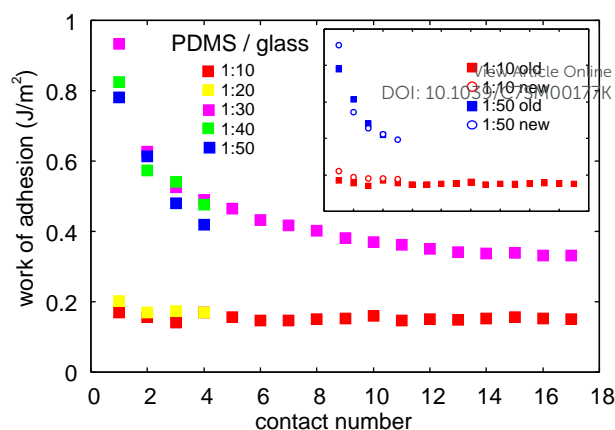


FIG. 8: The work of adhesion during retraction (separation) as a function of the number of contacts for all the PDMS compounds. The glass ball was originally cleaned with acetone but due to surface contamination by the uncrosslinked PDMS molecules, the adhesion decreases with the number of contacts. The effect is very large for the 1:50, 1:40 and 1:30 compound but rather small for the 1:20 and 1:10 compounds. In the insert we compare the work of adhesion for compounds 1:10 and 1:50 with measurements (open symbols) performed ~ 2 month later for the same compounds. The drive velocity is $v_z = 0.87 \mu\text{m/s}$.

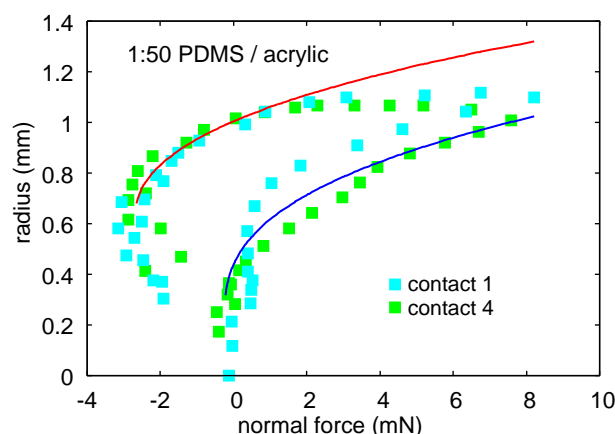


FIG. 9: The radius of the contact region as a function of normal force for an acrylic spherical probe (diameter $2R = 0.635 \text{ cm}$) during approach and retraction from a 1:50 Sylgard elastomer. The blue and green squares are measured data for contact cycle 1 and 4, respectively, and the blue and red lines are the JKR fit during retraction and approach, respectively. The drive velocity $v_z = \pm 0.475 \mu\text{m/s}$ and the crack tip velocity when the pull-off force is maximal $v_r = 1.78 \mu\text{m/s}$.

glass surface. For the 1:10 and 1:20 compounds the dependency of the work of adhesion on the contact number are much weaker. This suggests that these compounds have a much smaller amount of free PDMS molecules at the elastomer surfaces than the 1:30, 1:40 and 1:50 compounds. However, a small drop in the work of adhesion occurred also for the 1:10 and 1:20 compounds, which is

consistent with earlier studies[46–48].

For the acyclic ball we observed a much smaller change in the work of adhesion (or the pull-off force) with the number of contacts. This is illustrated in Fig. 9 for the 1:50 compound. We show the adhesion data for contact 1 (blue squares) and contact 4 (green squares). Within the noise of the experiment there was no change in the work of adhesion during retraction.

To understand this difference between the UF and Jülich experiments, note that the surface energy (per unit surface area) for glass cleaned by acetone (which results in a surface still covered by water and some organic contamination) is typically[49] $\gamma \approx 0.06\text{--}0.07\text{ J/m}^2$. The surface energy of the acrylic polymer is only[50] $\approx 0.03\text{ J/m}^2$, i.e., about half of that of the glass surface. The surface energy of PDMS[51] $\approx 0.02\text{ J/m}^2$ is similar to that of the acrylic polymer ball. Hence the probability for the acrylic ball to pick up PDMS molecules during contact with the PDMS is smaller than for the glass ball. Furthermore, if the acrylic ball gets covered by PDMS molecules it will have a relatively small influence on the surface energy of the ball, and hence on the adhesion force. Finally, we note that ethanol is not as strong a cleaning agent as acetone, and we cannot exclude that some PDMS molecules remains on the acrylic ball after cleaning the ball with ethanol.

In a simple approach one assumes that the adiabatic work of adhesion is [3] $w_0 = 2(\gamma_1\gamma_2)^{1/2}$ (where γ_1 and γ_2 are the surface energy of solids 1 and 2), which in the present case would give $w_0 \approx 0.04\text{ J/m}^2$ for PDMS against PDMS, $w_0 \approx 0.05\text{ J/m}^2$ for PDMS against clean acrylic polymer, and $w_0 \approx 0.08\text{ J/m}^2$ for PDMS against the glass surface. When pull-off occurs at a finite velocity the work of adhesion increases due to non-adiabatic effects. For the PDMS 1:10 against acrylic polymer we obtain the work of adhesion during pull-off (at the crack velocity $v_r \approx 2.5\text{ }\mu\text{m/s}$) to be about $w \approx 0.08\text{ J/m}^2$ (see Table I) (but this value is rather uncertain due to noise in the measured data), which is about 60% larger than expected in the adiabatic limit. For the same PDMS against glass we get the work of adhesion (at the crack velocity $v_r \approx 4\text{ }\mu\text{m/s}$) $w \approx 0.16\text{ J/m}^2$ (from Fig. 8), which is about $\sim 100\%$ larger than expected in the adiabatic limit. As will be shown below (see Sec. 4.5), for these cases the increase in the work of adhesion (compared to the adiabatic limit) can be explained as due to viscoelastic energy dissipation in front of the moving crack tip.

4.3 Dependence of the work of adhesion on the surface roughness

We now study how the adhesion depends on the surface roughness. This topic was also studied in a pioneering work by Fuller and Tabor[35]. Fig. 10 shows the logarithm of the work of adhesion during retraction (separation) as a function of the number of contacts for the 1:10 (red symbols) and the 1:50 (blue symbols) PDMS

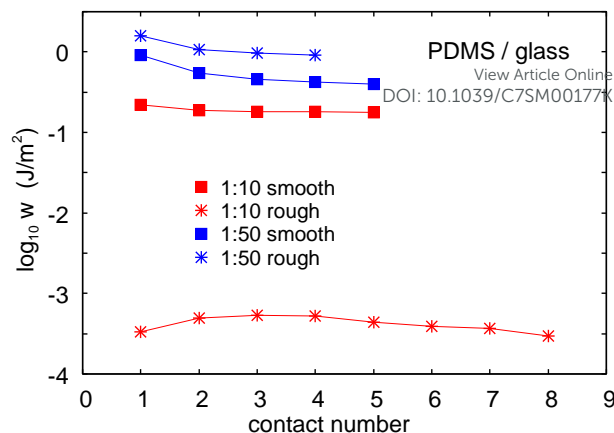


FIG. 10: The logarithm of the work of adhesion during retraction (separation) as a function of the number of contacts for the 1:10 (red symbols) and the 1:50 (blue symbols) PDMS compounds. The squares are for a glass ball with a smooth surface and the stars for a sand blasted glass surface. The glass balls were cleaned with acetone. The drive velocity is $v_z = 0.87\text{ }\mu\text{m/s}$.

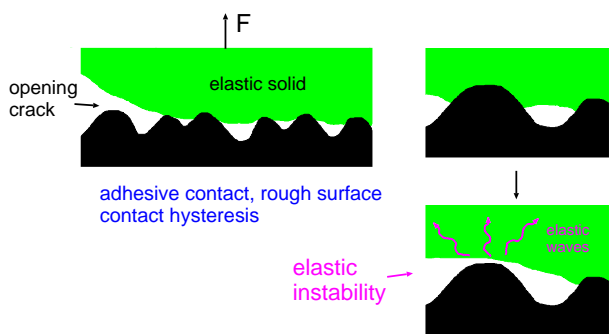


FIG. 11: Elastic instabilities close to the crack tip gives a contribution to the work of adhesion during pull-off.

compounds. The squares are for a smooth glass ball and the stars for a sand blasted glass ball. The glass balls were cleaned with acetone. Note the remarkable difference between the soft 1:50 elastomer and the stiffer 1:10 compound. For the stiff compound for the first contact the work of adhesion *decreases* from $\sim 0.2\text{ J/m}^2$ (smooth glass ball) to $\sim 3 \times 10^{-4}\text{ J/m}^2$ (rough glass ball) i.e. by a factor of ~ 700 . For the soft compound the work of adhesion instead *increases* from $\sim 0.9\text{ J/m}^2$ to $\sim 1.6\text{ J/m}^2$ i.e. by nearly a factor of ~ 2 .

For the stiff compound the drop in adhesion is due to the reduction in the contact area and due to the elastic energy stored at the interface when the elastomer surface deform locally to make contact with the rough surface[44]. During pull-off part of this elastic energy is “given back” and help to break the interfacial bonds. For the soft compound complete contact is likely to occur at the interface and very little elastic energy is stored at the interface because of the low value of the elastic modulus.

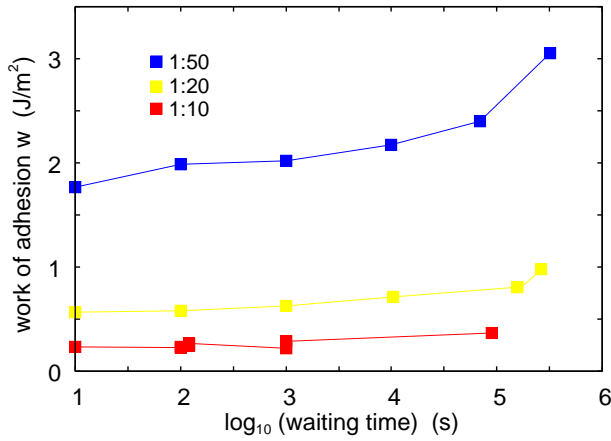


FIG. 12: The work of adhesion w as a function of the logarithm of the contact (waiting) time (i.e., the time of stationary contact) for the 1:10, 1:20 and 1:50 PDMS elastomers. The glass ball is loaded against the PDMS surface with the same force at time $t = 0$ and is removed with the same pull-off velocity $v_z \approx 50 \mu\text{m/s}$ in all cases.

Because of the surface roughness the area of contact between the glass and the elastomer is increased. We have measured the surface topography of the sandblasted surface using AFM but only for roughness with wavenumber $q < 0.1 \text{ nm}^{-1}$. If we extrapolate the power spectrum up to $q = 1 \text{ nm}^{-1}$ we calculate the ratio between the true surface area and the projected surface area $A_{\text{tot}}/A_0 \approx 1.7$ (and surface rms-slope 1.5), and the surface area would be even larger using an atomic cut-off $q = 2\pi/a \approx 10 \text{ nm}^{-1}$.

Another mechanism which results in an increase in the work of adhesion is due to surface roughness induced elastic instabilities (see Fig. 11)[52–56]. For perfectly smooth surfaces and for elastic solids (no viscoelasticity), the elastic energy stored ahead of a crack tip flows to the crack tip and is fully used to break the adhesive bonds at the crack tip. However, when surface roughness is present, local elastic instabilities may occur which result in fast local detachment events (see Fig. 11) at a velocity unrelated to the crack tip velocity. For elastic solids this leads to the emission of elastic waves (phonons) which will give rise to a contribution to the work of adhesion. It is not clear, however, how important such processes are in the present case.

4.4 Dependence of the work of adhesion on the contact time

It is well known that the strength of adhesive contacts usually increases with the time of stationary contact, e.g., due to slow (thermally induced) rearrangements of the atoms or molecules at the interface. One manifestation of this is an increase in the static (or beaklose) friction force with the time of stationary contact. This has a profound influence on sliding dynamics, as described by the Dieterich and Ruina rate and state dependent fric-

tion law[36, 37]. The increase in the breaklose friction force with the time of stationary contact is usually assumed to result from a slow (thermally activated) increase in the contact area[1]. However, recent studies have shown that formation of strong (covalent) bonds within the area of (atomic) contact, can also result in a slow (logarithmic in time) increase in the (adhesive and shear) strength of the contact region. Thus, for example, formation of siloxane bonds between silica surfaces has been suggested to result in an increase in the breaklose friction force with the time of stationary contact (chemical aging)[38, 39]. Similarly, Chaudhury and coworkers have observed time-dependent adhesion for PDMS with different surface treatment, which they attributed to the formation of hydrogen bonds between silanol groups at the interface[19].

We have studied how the work of adhesion (which is proportional to the pull-off force) depends on the time of stationary contact. Fig. 12 shows the work of adhesion w as a function of the logarithm of the contact time (i.e., the time of stationary contact) for the 1:10, 1:20 and 1:50 PDMS elastomers. The glass ball is loaded against the PDMS surface with the same force at time $t = 0$, and is removed with the same pull-off velocity $v_z \approx 50 \mu\text{m/s}$ in all cases. Before each experiment the glass ball was cleaned with acetone. Note that there is a slow increase in the work of adhesion, the exact origin of which we will not speculate. We note, however, that for the contact time intervals involved in the experiments performed in this study, the dependency of the work of adhesion on the time of stationary contact is rather small, and does not change any conclusions, e.g., related to the dependency of w on the crack speed (Sec. 4.5).

TABLE II: The critical crack tip velocity v_c and the exponent α of the $w \sim v^\alpha$ relation.

compound	v_c ($\mu\text{m/s}$)	exponent
1:20	6.3	0.50
1:30	0.13	0.34
1:40	0.063	0.34
1:50	0.013	0.28

4.5 Dependence of the work of adhesion on the pull-off velocity

The contact line between a spherical probe and a rubber substrate can be considered as a crack tip and the work of adhesion equals the crack propagation energy per unit surface area w . It is well known that the crack-propagation energy depends on the crack-tip velocity v and on the temperature T i.e. $w = w(v, T)$. In addition it differs for a closing crack and an opening crack.

The crack-propagation energy for an opening crack is

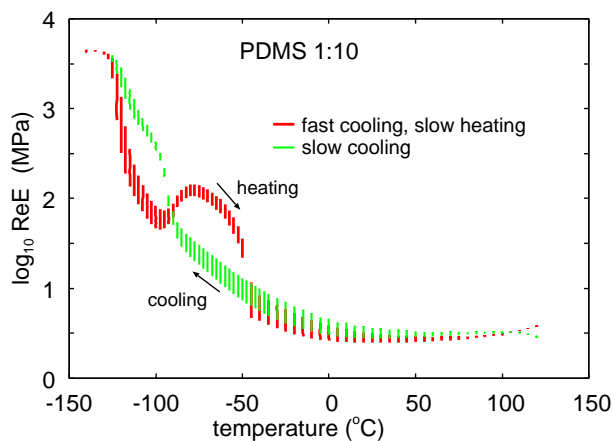


FIG. 13: The logarithm of the real part of the viscoelastic modulus, $\text{Re}E$, as a function of temperature T , for the PDMS 1:10 compound. The vertical lines are the E -modulus segments obtained when the frequency is varied between 0.25 Hz to 28 Hz. The red lines are the modulus obtained by first rapidly decreasing the temperature to -140 C, and then slowly increasing the temperature while measuring the viscoelastic frequency segments at different temperatures. The rapid cooling did not allow the elastomer to crystallize, but during heating up the elastomer did crystallize. The green lines were instead obtained by measuring the viscoelastic E -modulus segments at different temperatures during slow cooling of the elastomer from 120 C. In this case the elastomer crystallized at around -60 C.

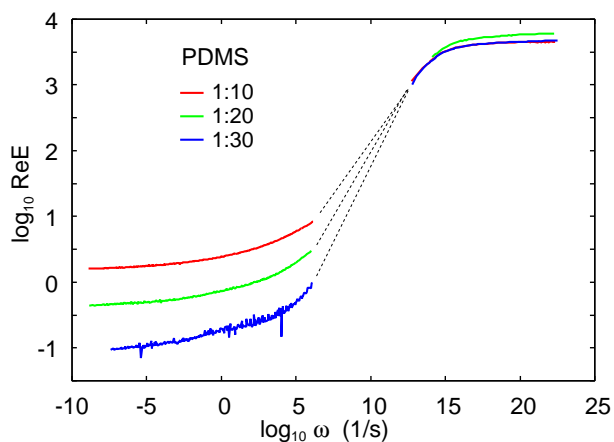


FIG. 14: The real part of the viscoelastic modulus, $\text{Re}E$ as a function of the angular frequency ω for the PDMS 1:10 (red line), 1:20 (green line) and 1:30 (blue line). The modulus was obtained using temperature-frequency shifting by first rapidly decreasing the temperature to -140 C and then slowly increasing the temperature while measuring the viscoelastic frequency segments at different temperatures separated by 5 C. The rapid cooling did not allow the elastomer to crystallize, but during heating up the elastomer crystallized when close (but below) to the melting temperature. The region where the crystallization occurs (and where the temperature-frequency shifting procedure fails) has been removed, and corresponds to the dotted lines.

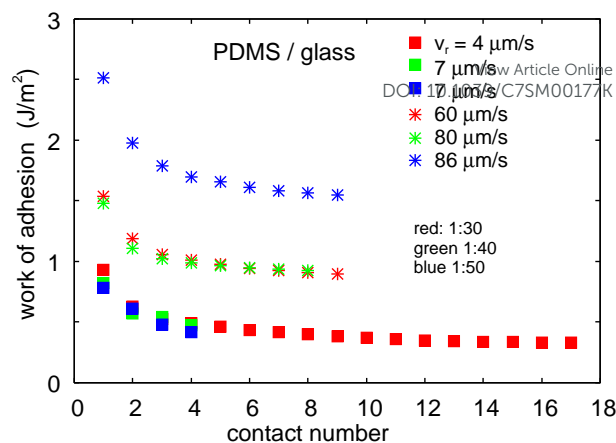


FIG. 15: The work of adhesion during retraction (separation) as a function of the number of contacts for the 1:50, 1:40 and 1:30 PDMS compounds. The glass ball was originally cleaned with acetone but due to surface contamination by the uncrosslinked PDMS molecules, the adhesion decreases with the number of contacts. Results are shown for the pull-off velocities $v_z = 35$ $\mu\text{m/s}$ (stars) and 0.87 $\mu\text{m/s}$ (squares) corresponding to typical crack velocities $v_r = 60 - 90$ $\mu\text{m/s}$ and $3 - 7$ $\mu\text{m/s}$, respectively.

often written as [40–43, 57]:

$$w(v, T) = w_0 [1 + f(v, T)]. \quad (5)$$

Here we are interested in interfacial (between the rubber and the substrate) crack propagation. In this case, as the crack velocity $v_r \rightarrow 0$ (when viscous effects in the rubber are negligible), the measured value of w_0 can be identified as the energy $w_0 = \gamma_1 + \gamma_2 - \gamma_{12}$ needed to break the interfacial rubber-substrate bonds, which are usually of the van der Waals type.

For simple hydrocarbon elastomers, the effect of temperature can be completely accounted for by applying a simple multiplying factor, denoted by a_T , to the crack velocity v , i.e., $f(v, T) = f(a_T v)$. Moreover, values of a_T found experimentally are equal to the Williams-Landel-Ferry (WLF) [58] function determined from the temperature dependence of the bulk viscoelastic modulus. This clearly proves that the large effects of crack velocity and temperature on crack propagation in rubber materials are due to the viscoelastic processes in the bulk.

In (5) the function $f(v, T) = f(a_T v)$ describes the bulk viscoelastic energy dissipation in front of the crack tip. This term is determined by the viscoelastic modulus $E(\omega)$ of the rubber, and can be calculated theoretically. The factor w_0 is due to the bond breaking (in our applications between the rubber and the substrate) at the crack tip (in the so-called *crack-tip process zone*), which may involve highly non-linear processes. This term cannot be calculated theoretically, and must be deduced directly from experimental data. The factor $f(v, T)$ in (5) may enhance w by a factor 10^3 or more at high crack-tip

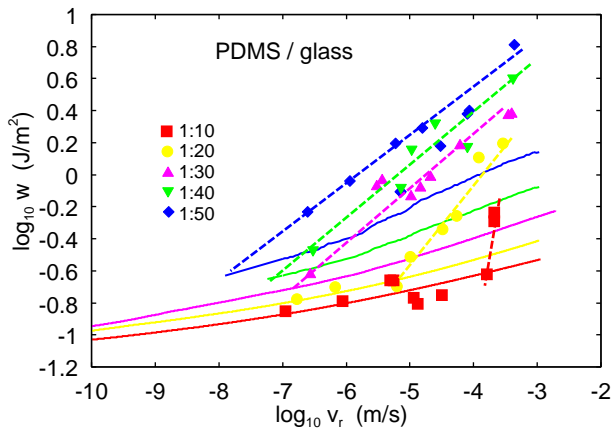


FIG. 16: The work of adhesion as a function of the crack tip velocity at the onset of instability (the point where the pull-off force is maximal). The different symbols are the measured data for the first contact between the glass ball and the 1:10 to 1:50 elastomers. The solid lines are the calculated crack propagation energy using (5)-(7) with $w_0 = 0.06 \text{ J/m}^2$. The calculation use the measured viscoelastic modulus for compounds 1:10, 1:20 and 1:30 and the results for compound 1:40 and 1:50 are obtained by extrapolation from the 1:10, 1:20 and 1:30 compounds. The dashed fit-lines cross the corresponding solid lines at the critical velocity v_c . Table II gives v_c and the slope of the dashed lines.

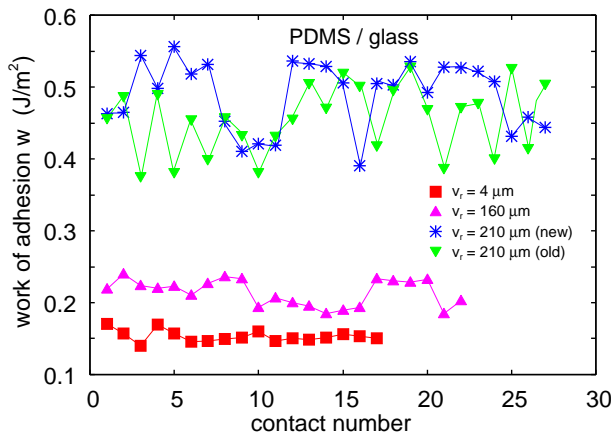


FIG. 17: The work of adhesion during retraction (separation) as a function of the number of contacts for the 1:10 PDMS compound. The glass ball was originally cleaned with acetone.

velocities.

In Ref. [23, 43] we have shown that

$$w(v) = w_0 \left[1 - \frac{2}{\pi} E_0 \int_0^{2\pi v/a} d\omega \frac{F(\omega)}{\omega} \text{Im} \frac{1}{E(\omega)} \right]^{-1} \quad (6)$$

where $E_0 = E(0)$ and where

$$F(\omega) = \left[1 - \left(\frac{\omega a}{2\pi v} \right)^2 \right]^{1/2}. \quad (7)$$

The crack tip radius $a = a(v)$ depends on the crack-tip

velocity v (and temperature), and can be determined if one assumes that the stress at the crack tip takes some critical value σ_c . This gives

DOI: 10.1039/C7SM00177K

$$\frac{a}{a_0} = \frac{w}{w_0} \quad (8)$$

where a_0 is the crack-tip radius for a very slowly moving crack taken to be $r_0 = 1 \text{ nm}$. For high crack-tip velocities $w(v) \approx w_0 E(\infty)/E(0) \gg w_0$. This is possible only if the denominator in the integral in (6) is close to zero for high crack-tip velocities which means that the term involving the integral must be close to unity. If (6) is used directly to calculate $w(v)$ numerically this requires that $E(\omega)$ is accurately known for all frequencies, which is usually not the case. However, it is possible to rewrite (6) in a form convenient for numerical calculations[23]. The predictions of the crack propagation theory presented above was compared to experimental data in Ref. [23, 43, 59–61]

Eq. (6) enables the prediction that for very high crack-tip speed the work of adhesion is increased by a factor of $E(\infty)/E(0)$, where $E(\infty)$ is the viscoelastic modulus for very high frequencies (in the glassy region) and $E(0)$ the static modulus. For rubber materials this factor is typically ~ 1000 . Since the elastic modulus of the PDMS elastomers 1:10 to 1:50 are nearly the same in the glassy region (see Fig. 14) (as expected from theory), and since in the rubbery region the viscoelastic modulus decreases with decreasing cross-link density (according to Table I by a factor of $\sim 0.019/2.3 \approx 0.01$ when going from the 1:10 elastomer to the 1:50 elastomer), it is clear that the contribution from the propagation of the opening crack will be larger for the 1:50 compound as compared to the 1:10 compound. This is confirmed by the calculations reported on below (see Fig. 16).

Many real rubber materials, in particular filled rubbers, exhibit non-linear rheological properties and the viscoelastic modulus $E(\omega)$, which enters in the crack propagation theory, should then be measured at a relatively large strain because the strain in the vicinity of a crack tip, or at an asperity contact region, will in general be very high (often of order 1).

In the present study we have measured the viscoelastic modulus of the 1:10, 1:20 and 1:30 PDMS elastomers. We find that when PDMS is slowly cooled it undergoes a (partial) crystallization at $T \approx -50^\circ\text{C}$. If crystallization occur one expects to observe hysteresis as the temperature is increased or decreased around the crystallization temperature. This is illustrated in Fig. 13 which shows the logarithm of the real part of the viscoelastic modulus, $\text{Re}E$, as a function of temperature T , for the PDMS 1:10 compound. The vertical lines are the E -modulus segments obtained when the frequency is varied between 0.25 Hz to 28 Hz. The red lines are the modulus obtained by first rapidly decreasing the temperature to -140°C , and then slowly increasing the temperature while mea-

asuring the viscoelastic frequency segments at different temperatures. The green lines was instead obtained by measuring the viscoelastic E -modulus segments at different temperatures during slow cooling of the elastomer from 120 C.

Fig. 14 shows the real part of the viscoelastic modulus, $\text{Re}E$, as a function of the angular frequency ω for the PDMS 1:10 (red line), 1:20 (green line) and 1:30 (blue line). The modulus was obtained using temperature-frequency shifting by first rapidly decreasing the temperature to -140°C , and then slowly increasing the temperature while measuring the viscoelastic frequency segments at different temperatures separated by 5°C . The rapid cooling did not allow the elastomer to crystallize, but during heating up the elastomer crystallize when close (but below) to the melting temperature. The region where the crystallization occur (and where the temperature-frequency shifting procedure fails) has been removed, and correspond to the dotted lines in Fig. 14. Using our DMA instrument we were not able to measure the viscoelastic mastercurve for the softer 1:40 and 1:50 PDMS compounds.

Note that in the JKR study the deformation rate is of order $\dot{r}(t)/r(t)$, which is of order 0.01 s^{-1} . From Fig. 14 for the frequency $\omega = 0.01\text{ s}^{-1}$ we obtain the elastic modulus $E \approx 2.2, 0.6$ and 0.16 MPa for the 1:10, 1:20 and 1:30 compound, respectively. The JKR analysis (see Table I) gave 2.3, 0.75 and 0.25 MPa which are slightly larger E -values than obtained from the DMA measurements. We note, however, that our measurement is for very small strain (0.04% strain) while the strain at pull-off in the ball-rubber contact region is of order $\delta(t)/r(t) \sim 0.1$ or 10% strain.

Using the modulus shown in Fig. 14 we have calculated the crack propagation energy using (5)-(8). In the studied velocity interval only the modulus in the rubbery-like (low-frequency) region before crystallization (i.e. before the dotted lines in Fig. 14) is used. The thick solid lines in Fig. 16 show the calculated work of adhesion at $T = 20^\circ\text{C}$ using $w_0 = 0.06\text{ J/m}^2$. The results for compound 1:40 and 1:50 were obtained by extrapolation from the 1:10, 1:20 and 1:30 compounds.

The different symbols are the measured data for the first contact between the glass ball and the 1:10 to 1:50 elastomers, at the crack tip velocity corresponding to the point where the pull-off force is maximal. In accordance with our earlier study[20], for the 1:10 compound the measured dependency of the work of adhesion on the crack tip velocity, $w = w(v)$, is in good agreement with the calculated result for $v < 100\text{ }\mu\text{m/s}$.

For the 1:20 compound the velocity data points for $v < 10\text{ }\mu\text{m/s}$ are in agreement with the calculation (yellow line), but the higher velocity data points occur at a much higher work of adhesion value than that predicted by the theory. In the study in Ref. [20] (where we measured w to higher velocities than in the present study),

and also in the present study we observed the same effect for the 1:10 compound for crack tip velocities above $100\text{ }\mu\text{m/s}$. This indicates that for low enough crack tip velocity the measured data for the 1:10 and 1:20 compounds follow the theory prediction, assuming that the velocity dependency of $w(v)$ is due only to the viscoelastic factor $f(v)$, but above some critical crack tip velocity, v_c , a new energy dissipation mechanism contributes, and results in a very fast increase of $w(v)$ with increasing crack tip velocity. This picture is supported by the data for the 1:30, 1:40 and 1:50 compounds in Fig. 16. For these compounds $w(v)$ increases very fast with increasing crack tip velocity v . Thus, the critical velocity v_c decreases with decreasing cross-link density.

We note that a fast increase in the crack propagation energy can result from the temperature increase in the vicinity of the crack tip due to the viscoelastic energy dissipation[62, 63]. However, at the low crack-tip velocities used in the present study, and the low crack propagation energy, this effect is negligible. Because of the low crack tip speed v thermal diffusion will spread out the crack propagation energy in a region in front of the crack tip with radius r determined by $r^2 = Dt$ where the time $t = r/v$, and where D is the heat diffusivity. Thus $r = D/v$. The heat diffusivity $D = \lambda/\rho c$ (where $\lambda \approx 0.1\text{ W/m}^2$ is the thermal conductivity, $\rho \approx 10^3\text{ kg/m}^3$ the mass density and $c \approx 10^3\text{ J/kgK}$ the heat capacity) so that $D \approx 10^{-7}\text{ m}^2/\text{s}$. Hence even at the highest speed in Fig. 16, $v \approx 10^{-3}\text{ m/s}$, we get $r \approx 1\text{ mm}$ i.e. similar to the radius of the JKR contact region. The temperature increase can be estimated using $wr^2 \approx \rho c \Delta T r^3$ or $\Delta T \approx w/(\rho c r) \approx wv/(\rho c D) = wv/\lambda \approx 0.01^\circ\text{C}$, which will have a negligible influence on the interfacial crack propagation.

The dashed lines in Fig. 16 are linear fit to the measured data for each PDMS compound in the logarithmic scale. The dashed lines cross the corresponding solid lines at the critical velocity v_c . Table II gives v_c and the slope of the dashed lines for the 1:20 to 1:50 compounds.

It is not clear if the enhancement effect with an onset at $v = v_c$ is due to the increased fraction of uncrosslinked PDMS chains, or due to the reduction in the (low-frequency) viscoelastic modulus with decreasing cross-link density. However, we note that the 1:50 compound has a similar (low-frequency) modulus as for pressure sensitive adhesives. For pressure sensitive adhesives the experiments have shown that cavitation and stringing occur in the contact area during separation, and result in a huge increase in the work of adhesion[22]. It is possible that similar processes contribute to the large work of adhesion in the present case, and that these processes only occur when the stresses at the interface are high enough, which require high enough crack tip velocities. However, inspection of the contact region for the acrylic ball case indicated a smooth circular and compact contact region, so most likely the increase in the work of

adhesion has another origin involving non-adiabatic processes during pull-off.

One possible mechanism of enhancement of the work of adhesion is associated with pull-out of non-crosslinked chains. If the chain pull-out occurs, it is likely that the glass ball gets contaminated with PDMS chains. Transfer of polymer chains to the glass ball clearly occurs for the 1:30, 1:40 and 1:50 compounds. However, this is not the case for the 1:10 compound even at the highest pull-off velocity where w is higher than predicted by the viscoelastic crack propagation theory (see Fig. 17). Fig. 17 shows the work of adhesion during retraction (separation) as a function of the number of contacts for the 1:10 PDMS compound for the three highest pull-off velocities (corresponding to the three highest (red square) crack-tip velocity data points in Fig. 16). Note that even for the two highest velocity data points there is no decrease in the adhesion with the number of contacts. Thus, for the 1:10 compound there is little support for the chain-pull out mechanism for the enhancement of w for $v > v_c$.

However, non-adiabatic processes may be also less drastic. For example, a segment of a polymer molecule may bind to the glass surface, gets stretched during pull-off, and flips back to the polymer surface as the bond to the glass surface breaks. At very low pull-off velocity the bond breaks due to the thermal fluctuations, and there would be no enhancement in the work of adhesion from this process. However, above some critical velocity $v > v_c = \delta/\tau$, where δ is some atomic distance and τ a relaxation time with an activated temperature dependency (τ decreases as the temperature increases), the polymer chain stretches before the glass-polymer bond break, and the elastic energy in the stretched polymer gets dissipated as heat when the bond breaks (non-adiabatic process)[24, 64]. If this picture is correct, the fact that v_c decreases as the crosslink density decreases implies that the relaxation time τ must increase with decreasing the crosslink density. Since $\tau = \tau_0 \exp(E_a/k_B T)$ this could be explained if the activation energy E_a involved in the bond-breaking increases when the crosslink density decreases. At first this may appear surprising since one expect higher mobility (i.e. lower energy barriers) of the PDMS chains in the less crosslinked compound. That is, in a more fluid-like material the material in the surrounding of a polymer chain can more easily adjust or displace away to lower the energy barriers for rearrangement of the polymer chains. However, the most important effect on E_a will be the interaction between the PDMS and the glass surface. If the glass surface immediately gets covered by PDMS molecules during the first contact with the PDMS sample, interdiffusion of PDMS chains between the PDMS surface and the PDMS covered glass ball may occur resulting in a possible enhanced effective E_a .

4.6 Work of adhesion for “extracted” Poly-



FIG. 18: The 1:30 PDMS elastomer after swelling in hexane and drying the sample.

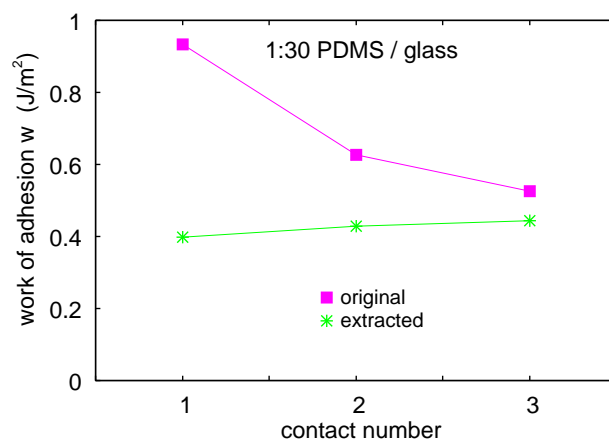


FIG. 19: The work of adhesion as a function of the number of contact for the 1:30 PDMS sample before extraction of the oligomers (pink squares) and after extraction (green stars). The drive velocity is $v_z = 0.87 \mu\text{m/s}$.

dimethylsiloxane

We have extracted the free chains (oligomers) from the 1:10, 1:30 and 1:50 PDMS elastomers by immersion in liquid hexane for 2-4 days (resulting in swelling) followed by drying for several days. After drying the 1:50 PDMS sample consisted of a large number of small fragments with irregular surfaces, and no adhesion experiments on this sample were possible. The 1:30 sample broke up into weakly coupled segments (layers), with cavities, and a highly irregular surface (see Fig. 18). Still we were able to perform adhesion measurements on the treated sample, but the work of adhesion is certainly influenced by the strong surface irregularities and the non-compact nature of the sample.

Fig. 19 shows the work of adhesion as a function of the number of contacts (at the pull-off speed $v_z = 0.9 \mu\text{m/s}$)

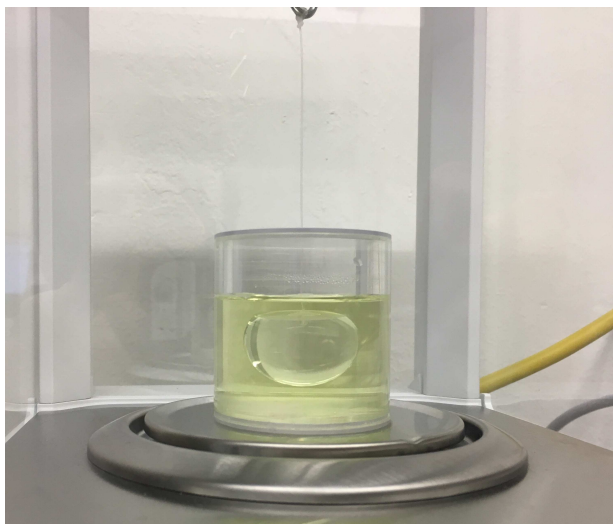


FIG. 20: Experimental set-up for adhesion studies in fluids (in this case water+soap; the light yellow fluid). The fluid is located in a Plexiglas container (inner diameter 4 cm) with a Plexiglas cover to avoid evaporation of the fluid. The top cover has a small hole (diameter 1 mm) through which the nylon rope (diameter 0.3 mm), used for moving the glass ball, passes. The elastomer sheet (in this case a transparent 1:30 PDMS sheet) is located at the bottom of the container. The glass ball (diameter 2.5 cm, with a flattened top part) is fully immersed in the fluid during the contact cycling. The container is located on a sensitive laboratory balance used for measuring the pull-off force.

for the treated sample, and the original (non-treated) 1:30 PDMS sample. Note that in contrast to the rapid drop in the work of adhesion for the non-treated sample, for the treated sample the work of adhesion is nearly independent of the contact number. This indicates that the fast drop in the work of adhesion for the non-treated sample is due to transfer of oligomers to the glass surface. It is also remarkable that in spite of the large surface roughness of the treated sample, the adhesion for the first contact is only a factor ~ 2 smaller than for the non-treated sample. This is due to the relatively low elastic modulus of the 1:30 PDMS elastomer. We note, however, that the quoted work of adhesion is not accurate for the treated sample as the condition for the validity of the JKR theory (homogeneous substrate with flat surface) is not obeyed. Still, the observation that the work of adhesion is nearly independent of the contact number is accurate as it does not depend on the validity of the JKR theory.

Due to the relatively small decrease in the mass (by $\sim 4\%$) of the treated 1:10 sample, it has a shape essentially unchanged from that of the original sample, and the work of adhesion for the treated sample is nearly independent of the number of contacts, just like for the non-treated sample. This is consistent with the low concentration of oligomers in the original (non-treated) sample.

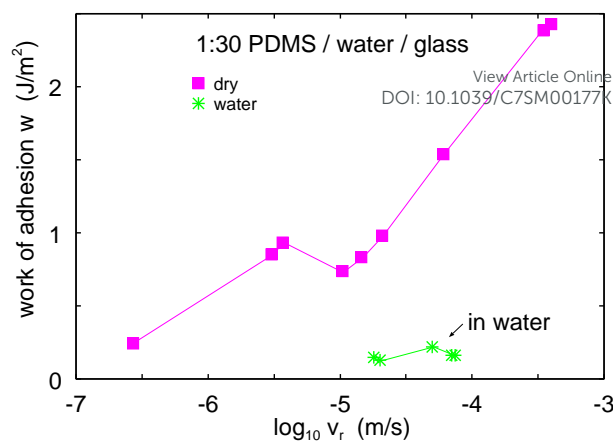


FIG. 21: The work of adhesion during retraction (separation) as a function of the logarithm of the crack tip speed. For 1:30 PDMS against glass for dry surfaces (squares) and in water (stars). The glass ball was cleaned with acetone before each measurement sequence.

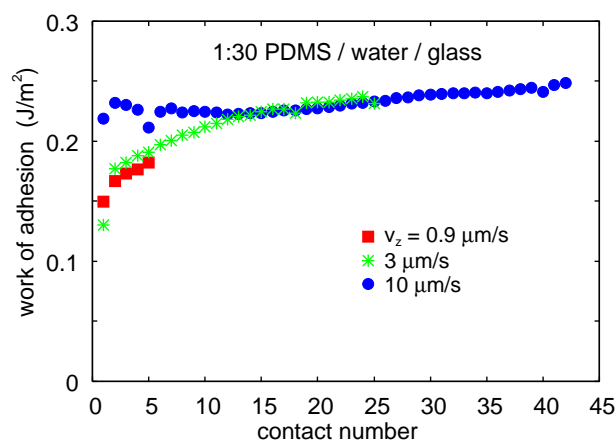


FIG. 22: The work of adhesion during retraction (separation) as a function of the number of contacts between 1:30 PDMS and glass in water. The glass ball was cleaned with acetone before each measurement sequence.

4.7 Work of adhesion in water

We have performed adhesion experiments for the 1:30 PDMS in water and in water + soap (see Fig. 20). In the latter case we do not observe any adhesion force during pull-off. This is indeed an expected result: the soap we use (a salt of a fatty acid) consists of hydrocarbon chain molecules with a head group which is *negatively* charged in water. In water the elastomer get covered by fatty acid molecules with the hydrocarbon chain towards the elastomer and the negative head group in the water (see Fig. 23(e)). The glass surface will spontaneously become negatively charged when immersed in water. This will result in an osmotic repulsion between the surfaces. Hence no pull-off force is expected in this case.

For the contact between the glass ball and the PDMS

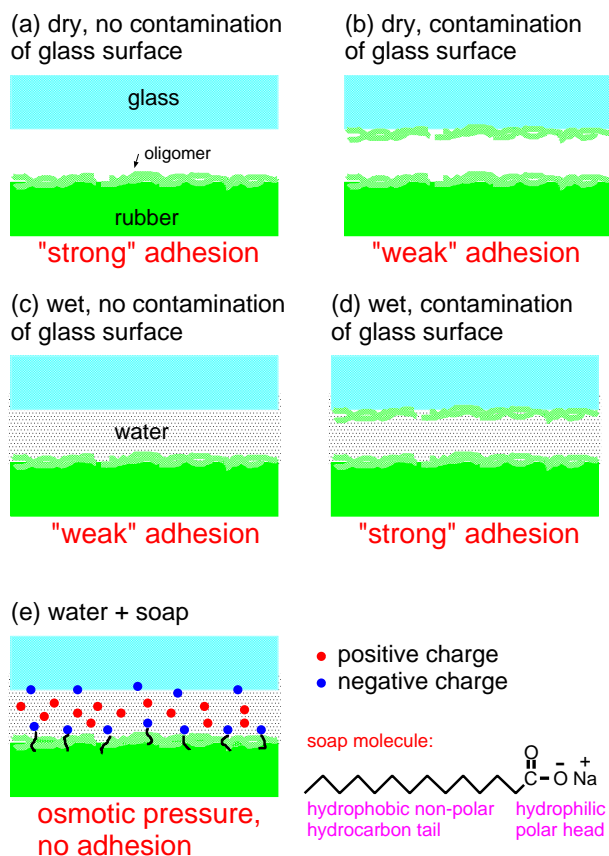


FIG. 23: For dry surfaces the work of adhesion decreases when the glass surface originally cleaned with acetone (a) becomes contaminated by transfer of PDMS oligomers (b). When the system is immersed in water the opposite effect occurs [see (c) and (d)]. This is due to the increased hydrophobicity of the contact upon transfer of PDMS oligomers to the glass surface. (e) For the PDMS-glass system in water+soap no adhesion is observed. This is due to the osmotic pressure associated with the negatively charged elastomer and glass surfaces.

in distilled water we observe adhesion, but the work of adhesion is about 5 times smaller than in the dry condition (see Fig. 21). Furthermore, while the work of adhesion in the dry state decreases rapidly with the number of contacts, we observe the opposite effect in water (see Fig. 22). We believe this is due to the following effect: if oligomers would be transferred to the glass surface during contact in water, this will lower the surface energy of the glass ball. Hence the glass ball will become more hydrophobic and the adhesion between hydrophobic surfaces in water is expected to be higher than between hydrophilic surfaces.

To understand this more quantitatively, note that the (adiabatic) work of adhesion in water can be written as

$$w(\text{wet}) = w(\text{dry}) - \gamma(\cos\theta_{\text{gw}} + \cos\theta_{\text{rw}}) \quad (9)$$

where $\gamma = 0.072 \text{ J/m}^2$ is the surface energy (or surface tension) of water, θ_{gw} the contact angle of water on glass

and θ_{rw} the contact angle of water on rubber. We assume $\theta_{\text{rw}} \approx 100^\circ$ and $w(\text{dry}) \approx 0.06 \text{ J/m}^2$ (see Sec. 4.5). In water the work of adhesion is about 15 times smaller than in air so the (adiabatic) work of adhesion $w(\text{wet}) \approx 0.012 \text{ J/m}^2$. Using (9) this implies that the contact angle $\theta_{\text{gw}} \approx 32^\circ$, which is very reasonable for the water-contact angle for glass surface cleaned with acetone (which still has strongly bound hydrocarbons). Now when the glass surface gets contaminated with PDMS oligomers the contact angle for water will increase, which according to (9) would tend to increase the work of adhesion. However, at the same time $w(\text{dry})$ decreases (maybe by a factor of 2 according to Fig. 8) but the experiments show that the increase in the water contact angle is more important. This result is plausible because if the glass surface would be covered by a thick PDMS film the work of adhesion $w(\text{dry})$ would drop from $\approx 0.06 \text{ J/m}^2$ to $\approx 0.04 \text{ J/m}^2$, while the water contact angle on the (contaminated) glass surface may increase from $\approx 32^\circ$ to $\approx 100^\circ$, so that the term $-\gamma(\cos\theta_{\text{gw}} + \cos\theta_{\text{rw}})$ would increase with $-\gamma(\cos(100^\circ) - \cos(30^\circ)) \approx 0.07 \text{ J/m}^2$. Thus, if the PDMS oligomer transfer film thickness increases with the number of contacts, we also expect the work of adhesion to increase with the number of contacts.

5 Experimental results for other rubber compounds

The PDMS samples studied above were very clean, and for the 1:10 compound there is only a low concentration of free molecules, which can diffuse to the surface and “contaminate” the surface. This is consistent with the adhesion measurements where we observed negligible changes in the adhesion with the number of contacts, even though ~ 5 hours occur between each contact. Even the 1:20 compound exhibits rather small changes in the work of adhesion with the number of contacts, indicating that for this compound too most of the chain molecules are crosslinked. For the softer compounds 1:30, 1:40 and 1:50 this is not the case and we observed a strong reduction in the adhesion with increasing number of contacts. We interpret this as resulting of transfer of “free” uncrosslinked rubber molecules to the glass surface resulting in an effective reduction in the glass ball surface energy, and a strong reduction in the work of adhesion with increasing number of contacts.

We now consider adhesion experiments for several other rubber compounds. These compounds were produced as sheets using high-pressure, high-temperature molding. In some cases release chemicals were used, which may form thin films on the rubber surface and influence the work of adhesion. The rubber surfaces have roughness to various degree related to the mold surface roughness. Polished steel surfaces are commonly used for the mold which may have surface roughness with a rms amplitude of order $\sim 0.1 \mu\text{m}$ or more. Thus these surfaces are not as smooth and clean as the PDMS surfaces

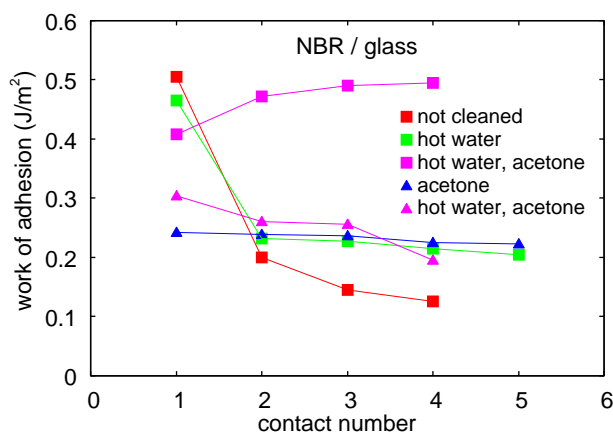


FIG. 24: The work of adhesion during retraction (separation) as a function of the number of contacts for the NBR rubber. The glass ball was cleaned with acetone before each measurement sequence. The rubber surface was either not cleaned (red squares), or cleaned by brushing the surface with a soft tooth brush for a few minutes in nearly boiling distilled water (green squares). The pink squares was when the rubber block which was cleaned in hot water, is cleaned further with acetone. The blue and pink triangles were obtained in measurements performed one month later for a rubber surface cleaned by acetone (blue) and in hot water followed by acetone (pink). The squares and triangles were measured on two different rubber surfaces. The drive velocity is $v_z = 0.87 \mu\text{m/s}$.

used in Sec. 4, which had negligible surface roughness (surface roughness from frozen capillary waves may exist but these are unimportant for the adhesion in the present case), and probably very little non-rubber contamination. For the adhesion experiments below we have, if nothing else is stated, cleaned the rubber surfaces by lapping the surfaces for a few seconds with a precision wipe wet by acetone.

5.1 Acrylonitrile Butadiene, Ethylene Propylene Diene, and polyepichlorohydrin elastomers

The NBR, EPDM and GECO elastomers studied in this section were vulcanized in the same mold and should have a similar roughness, derived from the mold. To minimize the role of additives, the rubbers were produced without any oil and filler particles, and the recipe includes only the following ingredients besides the rubber: activator (ZnO, Stearic acid), accelerators (CBS, TBzTD) and sulfur. The most probable effect on a change in the surface energy of the rubber samples comes from the stearic acid.

We have measured the water contact angles on the rubber surfaces from which one can estimate the surface energy using the Neumann's equation[65, 66], which gives $\gamma_1 = 35 \text{ mJ/m}^2$ for EPDM and NBR and 45 mJ/m^2 for the GECO elastomers. Thus we estimate the adiabatic work of adhesion $w_0 = 2(\gamma_1 \gamma_2)^{1/2}$ for all the compounds against glass to be in the range $\approx 0.09 - 0.1 \text{ J/m}^2$, where we have

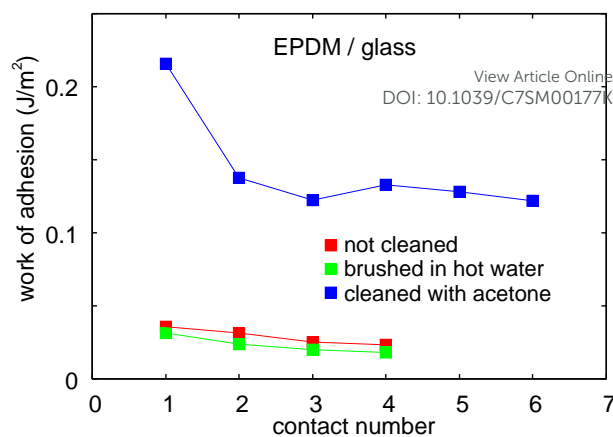


FIG. 25: The work of adhesion during retraction (separation) as a function of the number of contacts for the EPDM rubber. The glass ball was cleaned with acetone before each measurement sequence. The rubber surface was either not cleaned (red squares), or cleaned by brushing it with soft toothbrush in hot water (green squares) or cleaned with acetone (blue squares). The drive velocity is $v_z = 0.87 \mu\text{m/s}$.

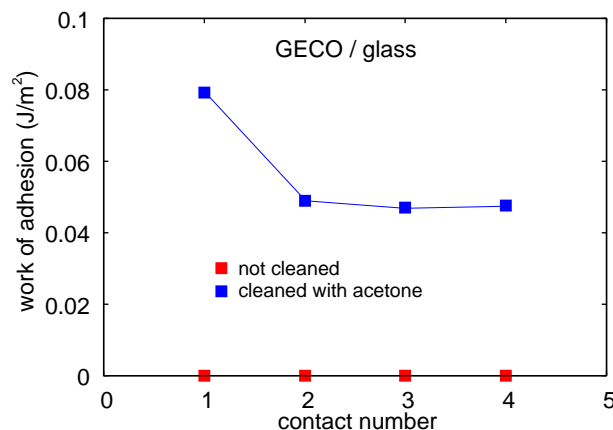


FIG. 26: The work of adhesion during retraction (separation) as a function of the number of contacts for the GECO rubber. The glass ball was cleaned with acetone before each measurement sequence. The rubber surface was either not cleaned (red squares), or cleaned with acetone (blue squares). The drive velocity is $v_z = 0.87 \mu\text{m/s}$.

assumed the glass ball surface energy $\gamma_2 = 60 \text{ mJ/m}^2$.

Most rubber compounds used in technology have many additives which can diffuse to the surface and result in a work of adhesion which change with time, temperature and the number of contacts. In our first study for a non-PDMS compound we have measured how the rubber adhesion depends on the surface cleaning procedure.

Fig. 24 shows the work of adhesion during retraction (separation) as a function of the number of contacts for the NBR elastomer. The glass ball was originally cleaned with acetone. The rubber surface was either not-cleaned (red squares), or cleaned by brushing the surface with a

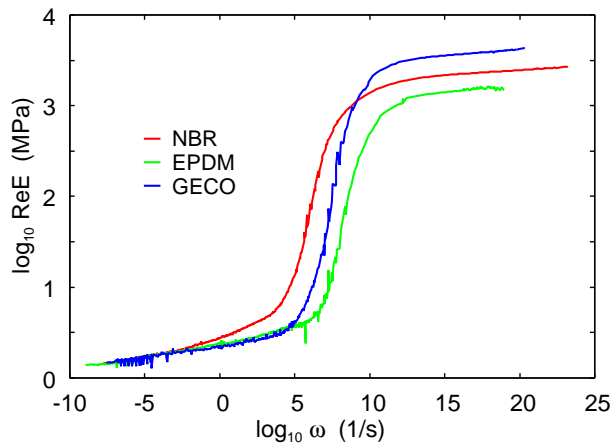


FIG. 27: The real part of the viscoelastic modulus for the NBR, EPDM and GECO elastomers, as a function of the frequency ω for $T = 20^\circ\text{C}$.

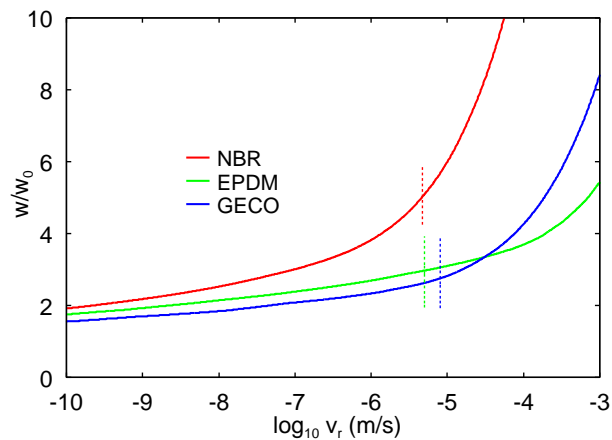


FIG. 28: The viscoelastic crack propagation factor $w/w_0 = 1 + f(v_r)$ as a function of the logarithm of the crack tip velocity v_r . For the the NBR, EPDM and GECO elastomers at $T = 20^\circ\text{C}$.

soft tooth brush for a few minutes in nearly boiling hot distilled water (green squares). The pink squares correspond to the rubber block, which was first cleaned in hot water for about 5 minutes, was cleaned further with acetone for a few seconds. The blue and pink triangles stand for the measurements performed one month later for a rubber surface cleaned by acetone (blue) and in hot water followed by acetone (pink). The squares and triangles were measured on two different rubber surfaces. We conclude that the non-cleaned rubber, and the rubber brushed in hot water, both have surface contamination which is transferred to the glass surface and result in decrease in the work of adhesion with the number of contacts. However, for the surface cleaned with acetone the adhesion stays nearly constant indicating that this surface is relatively clean to start with, and no or a negligible number of molecules diffuse to the surface during

the measurement. We note that the time interval between each contact is of order 5 hours.

In Fig. 25 and 26 we show the work of adhesion during retraction (separation) as a function of the number of contacts for the EPDM and GECO elastomers, respectively. In both cases we show results for non-cleaned (red squares) and for cleaned (with acetone) (blue squares) surfaces.

Note the huge variation in the work of adhesion in Fig. 24-26 in spite of the fact that the different rubber have very similar surface energies, and hence very similar adiabatic work of adhesion. Since the surface topography is the same (or nearly the same) in all cases, assuming it is determined by the roughness of the mold surface (which was the same for all the compounds), and since the low frequency viscoelastic modulus is nearly the same for all the rubbers (see Fig. 27), the difference must mainly be due to non-adiabatic effects e.g. different viscoelastic contribution to the crack propagation energy. In fact, we will now argue that the difference in the work of adhesion is mainly due to a combined action of surface roughness and viscoelastic enhancement of the crack propagation energy.

In Fig. 27 we show the real part of the viscoelastic modulus for the NBR, EPDM and GECO elastomers, as a function of the frequency ω for $T = 20^\circ\text{C}$. Using (5)-(8) we show in Fig. 28 the calculated viscoelastic crack propagation factor $w/w_0 = 1 + f(v)$ as a function of the logarithm of the crack tip velocity v at $T = 20^\circ\text{C}$. The three vertical dotted lines indicate the velocities of the crack tips at the point where the pull-off force is maximal for all three compounds. Thus, from the calculation we get the viscoelastic enhancement factors $w/w_0 \approx 5.1, 3.0$ and 2.6 for NBR, EPDM and GECO, respectively. If we assume the adiabatic work of adhesion $w_0 \approx 0.1 \text{ J/m}^2$ this gives $w \approx 0.51, 0.30$ and 0.26 J/m^2 for the NBR, EPDM and GECO elastomers, respectively. For the NBR elastomer this is similar to what is observed for contact number 1 but larger than observed for the EPDM and GECO elastomers. This can be understood as the influence of surface roughness on the adhesion. For elastic solids the adhesion is determined by the effective interfacial binding energy γ_{eff} determined by $\gamma_{\text{eff}} A_0 = \Delta\gamma A - U_{\text{el}}$, where $\Delta\gamma = \gamma_1 + \gamma_2 - \gamma_{12}$ is the binding energy for perfectly flat surfaces, and U_{el} is the elastic energy stored at the interface as a result of the deformations of the rubber surface necessary in order to make contact with the substrate. The area of real (atomic) contact and the nominal contact area are denoted by A and A_0 , respectively.

The elastic energy U_{el} depends on the surface roughness and the elastic properties of the solids, and vanishes for perfectly smooth surfaces. Since the low frequency elastic modulus is nearly the same for all three rubber compounds, we expect the U_{el} term to be similar too in all cases. Hence it follows that the elastic repulsion energy will result in a larger effect on the adhesion for the

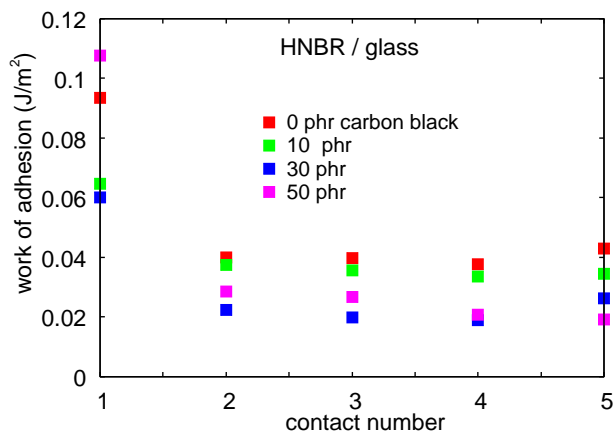


FIG. 29: The work of adhesion during retraction (separation) as a function of the number of contacts for HNB rubber. The glass ball was originally cleaned with acetone but due to surface contamination, the adhesion decreases with the number of contacts. The drive velocity is $v_z = 0.87 \mu\text{m/s}$.

EPDM and GECO elastomers, as compared to the NBR elastomer. This picture is supported by the observation that for the non-cleaned (contaminated) surfaces, where in general one expects the $\Delta\gamma$ to be reduced, the reduction in the adhesion is largest for the lowest-adhesion compound GECO. Thus for this compound it appears as if the binding energy term $\Delta\gamma A$ is nearly fully balanced by the repulsive elastic energy term U_{el} , resulting in the nearly vanishing adhesion observed in the experiments (see Fig. 26).

For viscoelastic solids the picture presented above for the influence of the elastic energy may not be so accurate, but qualitatively we believe we have presented the correct physical picture for what is observed. We also note that the viscoelastic contribution to crack propagation presented in Fig. 28 is based on the measured low strain viscoelastic modulus, but this may be a reasonable approximation for the unfilled compounds studied in this section.

TABLE III: The Young's modulus E at the frequency $f = 1$ Hz and the temperature $T = 20^\circ\text{C}$ for the HNBR elastomers with 0 phr, 10 phr, 30 phr and 50 phr carbon black filler. The low strain modulus (0.04% strain amplitude, linear response) and the effective modulus for 50% strain are shown. Note the strain softening for the filled compounds.

HNBR carbon filler	0 phr	10 phr	30 phr	50 phr
ReE [MPa], 0.04% strain	6.8	13.7	24.8	65.3
ReE [MPa], 50% strain	6.0	8.0	12.2	20.4
ImE [MPa], 0.04% strain	0.8	1.7	2.9	7.8
ImE [MPa], 50% strain	1.1	1.9	3.2	5.3

5.2 Hydrogenated Nitrile Butadiene elastomer

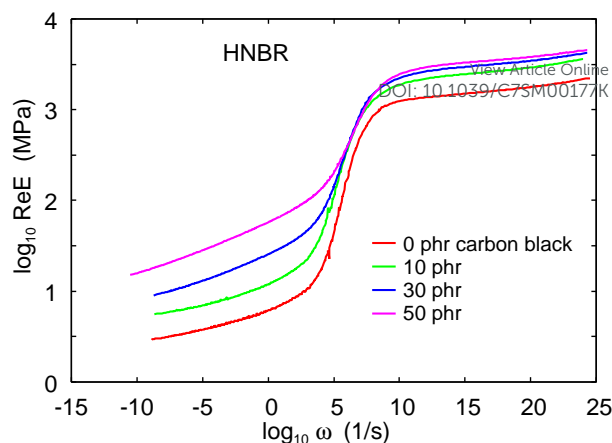


FIG. 30: The real part of the viscoelastic modulus for the HNB rubber compounds, as a function of the frequency ω for $T = 20^\circ\text{C}$.

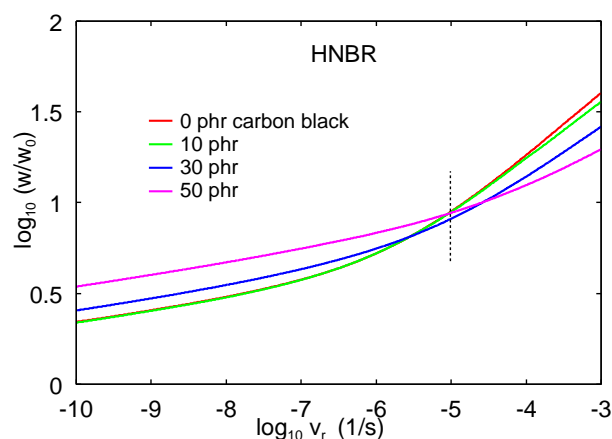


FIG. 31: The viscoelastic crack propagation factor $w/w_0 = 1 + f(v_r)$ as a function of the crack tip velocity v_r . For the HNB rubber compounds at $T = 20^\circ\text{C}$.

We have studied the adhesion between a glass ball and HNB rubber with different carbon filler concentration. Fig. 29 the work of adhesion during retraction (separation) as a function of the number of contacts. The results are shown for HNB rubber without filler (red line) and with 10 phr (green line), 30 phr (blue line) and 50 phr (pink line) carbon black filler. The glass ball was originally cleaned with acetone but due to transfer of molecules from the rubber to the glass surface, the latter got contaminated, and the effective surface energy was reduced, resulting in a decrease in the work of adhesion with the number of contacts.

Fig. 30 shows the real part of the viscoelastic modulus for the HNB rubber compounds, as a function of the frequency ω for $T = 20^\circ\text{C}$. In Fig. 31 we show the viscoelastic crack propagation factor $w/w_0 = 1 + f(v)$ as a function of the crack tip velocity v . Note that for the relevant crack velocity ($v_r \approx 10 \mu\text{m/s}$) (vertical dashed line) there

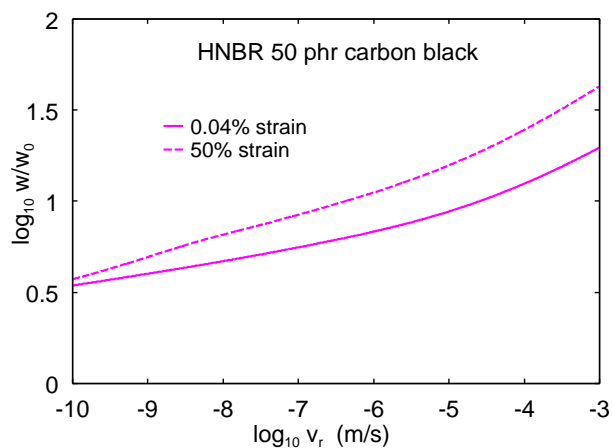


FIG. 32: The viscoelastic crack propagation factor $w/w_0 = 1+f(v)$ as a function of the crack tip velocity v . For the HNBR 50 phr carbon black filled rubber compounds at $T = 20^\circ\text{C}$. The solid line is obtained using the viscoelastic modulus measured at 0.04% strain and the dashed line using the effective modulus obtained at 50% strain. The strain softening results in a larger change in the modulus from the rubbery region to the glassy region, which in turn results in a larger crack propagation energy.

is a rather small difference in the calculated crack propagation energies and that $w/w_0 \approx 9$. Thus for perfectly smooth surfaces one would expect $w \approx 9w_0 \approx 0.9 \text{ J/m}^2$ where we have assumed the adiabatic work of adhesion $w_0 = 0.1 \text{ J/m}^2$. This is much larger than observed experimentally, indicating the importance of the surface roughness in reducing the work of adhesion. All the rubber surfaces were produced by molding against the same smooth (polished) steel surface, and are likely to have the same surface roughness. Thus, since the elastic energy U_{el} is proportional to the (low frequency) elastic modulus, which is much larger for the 50 phr compound compared to the 0 phr compound, one would expect a much larger influence on the adhesion by the surface roughness for the 50 phr compound as compared to the 0 phr compound. This is not observed, and we will now address this problem.

The viscoelastic modulus in Fig. 30 was obtained at the strain amplitude 0.04%. As shown in Table III at this strain amplitude the elastic modulus at the frequency $f = 1 \text{ Hz}$ is almost 10 times higher for the 50 phr carbon black compound compared to the 0 phr compound. However, the strain at the crack tip and in the asperity contact regions are much higher than 0.04%.

Most filled rubber compounds are known to strongly soften when the strain is above $\sim 1\%$. This effect is associated with the breakup of the filler network, and result in an effective modulus which (for filled compounds) may be a factor 3-5 lower than in the small strain limit. This is illustrated in Table III. Note that the 0 phr compound exhibit negligible strain softening, while the modulus of

the 50 phr compound drop by a factor of 3.3. Thus at the strain amplitudes of relevance the low frequency elastic modulus of the 0 phr and 50 phr compounds differ only by a factor of ~ 3 . This strain softening has two effects: it reduces the elastic energy U_{el} for the filled compounds and it tends to increase the crack propagation energy for the filled compounds. The latter is illustrated in Fig. 32 for the 50 phr compound. At the crack tip velocity $v_r = 10 \mu\text{m/s}$, the ratio w/w_0 increases from 9 to 16. We believe it is a combination of the decrease in U_{el} (as a result of the decrease in the viscoelastic modulus) and an increase in the crack propagation energy which result in the relatively small change in the work of adhesion with the filler concentration.

6 Summary and conclusion

We have studied adhesion characteristics of diverse elastomers having different chemical and viscoelastic properties. The results were analyzed using the JKR theory. We used elastomers such as PDMS (with varying crosslink density), NBR, EPDM, GECCO, HNBR (with varying carbon black filler). Glass and acrylic balls were made to come in repeated contact with these substrates.

For PDMS based elastomers, we observed that the surface roughness of the glass ball has a different effect on the work of adhesion depending on the elasticity of the PDMS substrate. For the stiff PDMS substrate the work of adhesion is reduced by a factor of ~ 700 for the rough glass ball as compared to the smooth one. For the soft PDMS substrate the work of adhesion instead increases by a factor of ~ 2 for the rough glass ball. All the PDMS elastomers showed the increased work of adhesion with increasing crack tip velocity. For the 1:10 and 1:20 PDMS compounds, below some critical crack tip velocity (v_c) the work of adhesion was reasonably well predicted by viscoelastic crack propagation theory. Above the critical crack tip velocity v_c the work of adhesion increased drastically for all the PDMS compounds. The critical crack tip velocity v_c is lower for the compounds with lower crosslink density. The increased work of adhesion with increasing velocities was more prominent in softer PDMS compounds 1:30 to 1:50.

The work of adhesion obtained from experiments carried out in air (i.e. dry) and water (i.e. wet) as a function of number of contacts showed completely opposite behaviour. In air, the work of adhesion decreases by a factor of 2 and in water it shows an increasing trend. The transfer of PDMS oligomers from the PDMS surface to glass ball surface was found to modify the surface energy of the glass ball making it more hydrophobic and this increased hydrophobicity led to an increase in work of adhesion in wet environments as compared to dry environments.

For other elastomers used in the study the work of adhesion was mainly governed by factors such as clean-

ing method, presence of contaminants on the surface and roughness of the rubber substrate. For filled compound with varying filler content, strain softening of the filled rubber at the crack tip plays a role in the work of adhesion.

We have distinguished the three major contributions to rubber adhesion acting at different length scales: bulk viscoelasticity, roughness and molecular mobility. The time-dependent viscoelastic contribution leads to higher adhesion for the softer compounds at the same velocities. The roughness contribution can have different sign depending on the stiffness of the rubber compound. This different behavior can be explained by the additional elastic energy stored while contact formation of the stiffer rubber with the rough surface and the additional contact area in the case of the compliant softer rubber. Mobile molecules in the weakly cross-linked structures can get attached to the countersurface and are pulled out from the substrate accompanied with energy dissipation and the increased work of adhesion.

Acknowledgments: We thank M.K. Chaudhury for useful discussions. This work was performed within a Reinhart-Koselleck project funded by the Deutsche Forschungsgemeinschaft (DFG). We would like to thank DFG for the project support under the reference German Research Foundation DFG-Grant: MU 1225/36-1. The research work was also supported by the DFG-grant: PE 807/10-1 and DFG-grant No. HE 4466/34-1. This work is supported in part by the Research Council of Norway (Project 234115 in the Petromaks2 programme). This work is supported in part by COST Action MP1303.

-
- [1] Persson, B. Sliding Friction: Physical Principles and Applications. Springer Science & Business Media: 2013.
- [2] Gnecco, E.; Meyer, E. Elements of Friction Theory and Nanotribology. Cambridge University Press: 2015.
- [3] Israelachvili, J. N. Intermolecular and Surface Forces: Revised Third Edition. Academic press: 2011.
- [4] Persson, B. N. J. Contact Mechanics for Randomly Rough Surfaces. Surface Science Reports 2006, 61, 201-227.
- [5] Hyun, S.; Pei, L.; Molinari, J. F.; Robbins, M. O. Finite-Element Analysis of Contact between Elastic Self-Affine Surfaces. Physical Review E 2004, 70, 026117.
- [6] Campana, C.; Müser, M. H. Contact Mechanics of Real Vs. Randomly Rough Surfaces: A Green's Function Molecular Dynamics Study. EPL (Europhysics Letters) 2007, 77, 38005.
- [7] Dapp, W. B.; Lücke, A.; Persson, B. N. J.; Müser, M. H. Self-Affine Elastic Contacts: Percolation and Leakage. Phys Rev Lett 2012, 108, 244301.
- [8] Persson, B. N. J. Theory of Rubber Friction and Contact Mechanics. The Journal of Chemical Physics 2001, 115, 3840-3861.
- [9] Akarapu, S.; Sharp, T.; Robbins, M. O. Stiffness of Contacts between Rough Surfaces. Phys Rev Lett 2011, 106, 204301.
- [10] Campana, C.; Persson, B. N. J.; Müser, M. H. Transverse and Normal Interfacial Stiffness of Solids with Randomly Rough Surfaces. Journal of Physics: Condensed Matter 2011, 23, 085001.
- [11] Pastewka, L.; Robbins, M. O. Contact between Rough Surfaces and a Criterion for Macroscopic Adhesion. Proceedings of the National Academy of Sciences 2014, 111, 3298-3303.
- [12] Persson, B. N. J.; Sivebaek, I. M.; Samoilov, V. N.; Ke, Z.; Volokitin, A. I.; Zhenyu, Z. On the Origin of Amonton's Friction law. Journal of Physics: Condensed Matter 2008, 20, 395006.
- [13] Carbone, G.; Scaraggi, M.; Tartaglino, U. Adhesive Contact of Rough Surfaces: Comparison between Numerical Calculations and Analytical Theories. The European Physical Journal E 2009, 30, 65.
- [14] Chateauminois, A.; Fretigny, C. Local Friction at a Sliding Interface between an Elastomer and a Rigid Spherical Probe. The European Physical Journal E 2008, 27, 221.
- [15] Newby, B.-m. Z.; Chaudhury, M. K.; Brown, H. R. Macroscopic Evidence of the Effect of Interfacial Slippage on Adhesion. Science 1995, 269, 1407-1409.
- [16] Schmidt, D. L.; Brady, R. F.; Lam, K.; Schmidt, D. C.; Chaudhury, M. K. Contact Angle Hysteresis, Adhesion, and Marine Biofouling. Langmuir 2004, 20, 2830-2836.
- [17] Chaudhury, M. K. Interfacial Interaction between Low-Energy Surfaces. Materials Science and Engineering: R: Reports 1996, 16, 97-159.
- [18] Silberzan, P.; Perutz, S.; Kramer, E. J.; Chaudhury, M. K. Study of the Self-Adhesion Hysteresis of a Siloxane Elastomer Using the Jkr Method. Langmuir 1994, 10, 2466-2470.
- [19] Ghatak, A.; Vorvolakos, K.; She, H.; Malotky, D. L.; Chaudhury, M. K. Interfacial Rate Processes in Adhesion and Friction. The Journal of Physical Chemistry B 2000, 104, 4018-4030.
- [20] Lorenz, B.; Krick, B.; Mulakaluri, N.; Smolyakova, M.; Dieluweit, S.; Sawyer, W.; Persson, B. Adhesion: Role of Bulk Viscoelasticity and Surface Roughness. Journal of Physics: Condensed Matter 2013, 25, 225004.
- [21] Krick, B. A.; Vail, J. R.; Persson, B. N. J.; Sawyer, W. G. Optical in Situ Micro Tribometer for Analysis of Real Contact Area for Contact Mechanics, Adhesion, and Sliding Experiments. Tribology Letters 2012, 45, 185-194.
- [22] Creton, C.; Ciccotti, M. Fracture and Adhesion of Soft Materials: A Review. Reports on Progress in Physics 2016, 79, 046601.
- [23] Persson, B. N. J.; Albohr, O.; Heinrich, G.; Ueba, H. Crack Propagation in Rubber-Like Materials. Journal of Physics: Condensed Matter 2005, 17, R1071.
- [24] Kendall, K. More Intricate Mechanisms: Raising and Lowering Adhesion. Molecular Adhesion and Its Applications: The Sticky Universe 2001, 155-178.
- [25] Persson, B. N. J.; Albohr, O.; Tartaglino, U.; Volokitin, A. I.; Tosatti, E. On the Nature of Surface Roughness with Application to Contact Mechanics, Sealing, Rubber Friction and Adhesion. Journal of Physics: Condensed Matter 2005, 17, R1.
- [26] Persson, B. N. J.; Scaraggi, M. Theory of Adhesion: Role of Surface Roughness. The Journal of Chemical Physics 2014, 141, 124701.
- [27] Persson, B. N. J. Silicone Rubber Adhesion and Sliding

- Friction. *Tribology Letters* 2016, 62, 34.
- [28] Persson, B. N. J. On the Mechanism of Adhesion in Biological Systems. *The Journal of Chemical Physics* 2003, 118, 7614-7621.
- [29] Arzt, E.; Gorb, S.; Spolenak, R. From Micro to Nano Contacts in Biological Attachment Devices. *Proceedings of the National Academy of Sciences* 2003, 100, 10603-10606.
- [30] Persson, B. N. J.; Gorb, S. The Effect of Surface Roughness on the Adhesion of Elastic Plates with Application to Biological Systems. *The Journal of Chemical Physics* 2003, 119, 11437-11444.
- [31] Nase, J.; Ramos, O.; Creton, C.; Lindner, A. Debonding Energy of Pdms. *The European Physical Journal E* 2013, 36, 103.
- [32] Johnson, K. L.; Kendall, K.; Roberts, A. D. Surface Energy and the Contact of Elastic Solids. *Proceedings of the Royal Society of London. A. Mathematical and Physical Sciences* 1971, 324, 301-313.
- [33] Deruelle, M.; Hervet, H.; Jandeau, G.; Lger, L. Some Remarks on Jkr Experiments. *Journal of Adhesion Science and Technology* 1998, 12, 225-247.
- [34] Derjaguin, B. V.; Muller, V. M.; Toporov, Y. P. Effect of Contact Deformations on the Adhesion of Particles. *Journal of Colloid and Interface Science* 1975, 53, 314-326.
- [35] Fuller, K. N. G.; Tabor, D. The Effect of Surface Roughness on the Adhesion of Elastic Solids. *Proceedings of the Royal Society of London. A. Mathematical and Physical Sciences* 1975, 345, 327-342.
- [36] Dieterich, J. H. Time-Dependent Friction and the Mechanics of Stick-Slip. *pure and applied geophysics* 1978, 116, 790-806.
- [37] Ruina, A. Slip Instability and State Variable Friction Laws. *Journal of Geophysical Research: Solid Earth* 1983, 88, 10359-10370.
- [38] Liu, Y.; Szlufarska, I. Chemical Origins of Frictional Aging. *Phys Rev Lett* 2012, 109, 186102.
- [39] K. Tian, N.N. Gosvami, D.L. Goldsby, Y. Liu, I. Szlufarska, and R.W. Carpick, Load and Time Dependence of Interfacial Chemical Bond-Induced Friction at the Nanoscale *Phys. Rev. Lett.* 2017, 118, 076103
- [40] Greenwood, J. A. The Theory of Viscoelastic Crack Propagation and Healing. *Journal of Physics D: Applied Physics* 2004, 37, 2557.
- [41] Greenwood, J. A. Viscoelastic Crack Propagation and Closing with Lennard-Jones Surface Forces. *Journal of Physics D: Applied Physics* 2007, 40, 1769.
- [42] Greenwood, J. A.; Johnson, K. L.; Choi, S. H.; Chaudhury, M. K. Investigation of Adhesion Hysteresis between Rubber and Glass Using a Pendulum. *Journal of Physics D: Applied Physics* 2009, 42, 035301.
- [43] Persson, B. N. J.; Brener, E. A. Crack Propagation in Viscoelastic Solids. *Physical Review E* 2005, 71, 036123.
- [44] Persson, B. N. J. Adhesion between an Elastic Body and a Randomly Rough Hard Surface. *The European Physical Journal E* 2002, 8, 385-401.
- [45] Barthel, E.; Frtigny, C. Adhesive Contact of Elastomers: Effective Adhesion Energy and Creep Function. *Journal of Physics D: Applied Physics* 2009, 42, 195302.
- [46] Kroner, E.; Maboudian, R.; Arzt, E. Adhesion Characteristics of Pdms Surfaces During Repeated Pull-Off Force Measurements. *Advanced Engineering Materials* 2010, 12, 398-404.
- [47] Kroner, E.; Maboudian, R.; Arzt, E. Effect of Repeated Contact on Adhesion Measurements Involving Polydimethylsiloxane Structural Material. *ICP Conference Series: Materials Science and Engineering* 2009, 5, 012004.
- [48] Kroner, E.; Paretkar, D. R.; McMeeking, R. M.; Arzt, E. Adhesion of Flat and Structured Pdms Samples to Spherical and Flat Probes: A Comparative Study. *The Journal of Adhesion* 2011, 87, 447-465.
- [49] The surface energy per unit surface area for soda-lime glass is about $\gamma \approx 0.3 \text{ J/m}^2$, as obtained by extrapolating the surface tension of melted glass to $T = 300 \text{ K}$ (see Shartsis, L.; Spinner, S. Surface Tension of Molten Alkali Silicates. *Journal of Research of the National Bureau of Standards* 1951, 46, 385-390). However, glass surfaces cleaned with acetone still have some strongly bounded organic contamination (and water) which lowers the surface energy to $0.06 - 0.07 \text{ J/m}^2$. The organic contamination can be removed by oxygen plasma or pirania solution, but when the glass is kept in the normal atmosphere it quickly get passivated by organic contamination. The glass surfaces in our study was cleaned only with acetone.
- [50] See, e.g.: <http://www.surface-tension.de/solid-surface-energy.htm>
- [51] Chaudhury, M. K.; Whitesides, G. M. Direct Measurement of Interfacial Interactions between Semispherical Lenses and Flat Sheets of Poly(Dimethylsiloxane) and Their Chemical Derivatives. *Langmuir* 1991, 7, 1013-1025.
- [52] Zilberman, S.; Persson, B. N. J. Nanoadhesion of Elastic Bodies: Roughness and Temperature Effects. *The Journal of Chemical Physics* 2003, 118, 6473-6480.
- [53] Li, Q.; Kim, K.-S. Micromechanics of Rough Surface Adhesion: A Homogenized Projection Method. *Acta Mechanica Sinica* 2009, 22, 377-390.
- [54] Mulakaluri, N.; Persson, B. N. J. Adhesion between Elastic Solids with Randomly Rough Surfaces: Comparison of Analytical Theory with Molecular-Dynamics Simulations. *EPL (Europhysics Letters)* 2011, 96, 66003.
- [55] Carbone, G.; Pierro, E.; Recchia, G. Loading-Unloading Hysteresis Loop of Randomly Rough Adhesive Contacts. *Physical Review E* 2015, 92, 062404.
- [56] Müser, M. H. A Dimensionless Measure for Adhesion and Effects of the Range of Adhesion in Contacts of Nominally Flat Surfaces. *Tribology International* 2016, 100, 41-47.
- [57] Maugis, D.; Barquins, M. Fracture Mechanics and the Adherence of Viscoelastic Bodies. *Journal of Physics D: Applied Physics* 1978, 11, 1989.
- [58] Williams, M. L.; Landel, R. F.; Ferry, J. D. The Temperature Dependence of Relaxation Mechanisms in Amorphous Polymers and Other Glass-Forming Liquids. *Journal of the American Chemical Society* 1955, 77, 3701-3707.
- [59] Morishita, Y.; Tsunoda, K.; Urayama, K. Velocity Transition in the Crack Growth Dynamics of Filled Elastomers: Contributions of Nonlinear Viscoelasticity. *Physical Review E* 2016, 93, 043001.
- [60] Morishita, Y.; Tsunoda, K.; Urayama, K. Crack-Tip Shape in the Crack-Growth Rate Transition of Filled Elastomers. *Polymer* 2017, 108, 230-241.
- [61] Sun, T. L.; Luo, F.; Hong, W.; Cui, K.; Huang, Y.; Zhang, H. J.; King D. R.; Kurokawa, T.; Nakajima, T.; Gong, J. P. Bulk Energy Dissipa-

- tion Mechanism for the Fracture of Tough and Self-Healing Hydrogels. *Macromolecules* 2017, in press, DOI: 10.1021/acs.macromol.7b00162.
- [62] Carbone, G; Persson, BNJ. Crack motion in viscoelastic solids: The role of the flash temperature *EUROPEAN PHYSICAL JOURNAL E* 2005, 17, 261-281.
- [63] Carbone, G; Persson, BNJ. Hot cracks in rubber: Origin of the giant toughness of rubberlike materials By: Carbone, G; Persson, BNJ *PHYSICAL REVIEW LETTERS* 2005, 95, 114301.
- [64] Thanawala, S. K.; Chaudhury, M. K. Surface Modification of Silicone Elastomer Using Perfluorinated Ether. *Langmuir* 2000, 16, 1256-1260.
- [65] Li, D.; Neumann, A. Equation of State for Interfacial Tensions of Solid-Liquid Systems. *Advances in Colloid and Interface Science* 1992, 39, 299-345.
- [66] Stöckelhuber, K. W.; Das, A.; Jurk, R.; Heinrich, G. Contribution of Physico-Chemical Properties of Interfaces on Dispersibility, Adhesion and Flocculation of Filler Particles in Rubber. *Polymer* 2010, 51, 1954-1963.

View Article Online
DOI: 10.1039/C7SM00177K

The interplay of viscoelasticity, surface roughness and molecular mobility on rubber adhesion is investigated experimentally and supported by theoretical analysis.

View Article Online

DOI: 10.1039/C7SM00177K

